MASS 2023 Course:

Gravitational Lenses

Predrag Jovanović

Astronomical Observatory Belgrade

Lecture 11

1. Influence of gravitational microlensing on AGN emission in different spectral bands and its applications for studying the physics around the central SMBHs of AGN
   - Simulations of X-ray radiation from relativistic accretion disks around SMBHs based on ray-tracing method in Kerr metric
   - Simple microlens models (point-like, straight-fold caustic and microlensing magnification map) and their effects on AGN emission
   - X-ray variability of AGN in the Fe Kα line and X-ray continuum due to microlensing
   - Microlensing of lensed quasars and flux anomaly
   - Chromatic effects of gravitational microlensing
   - Microlensing timescales and simulated light curves
   - Microlensing of extended sources
2. Optical depth and statistics of strong lenses
   - Constraints on the cosmological parameters from strong lensing statistics
3. Exercises

Central SMBHs of Active Galaxies

- Active galaxies are up to 10,000 times brighter than normal galaxies
- Small very bright core embedded in an otherwise typical galaxy

Left: NGC 5548 (Seyfert galalaxy)

Right: NGC 3277 (regular galaxy)

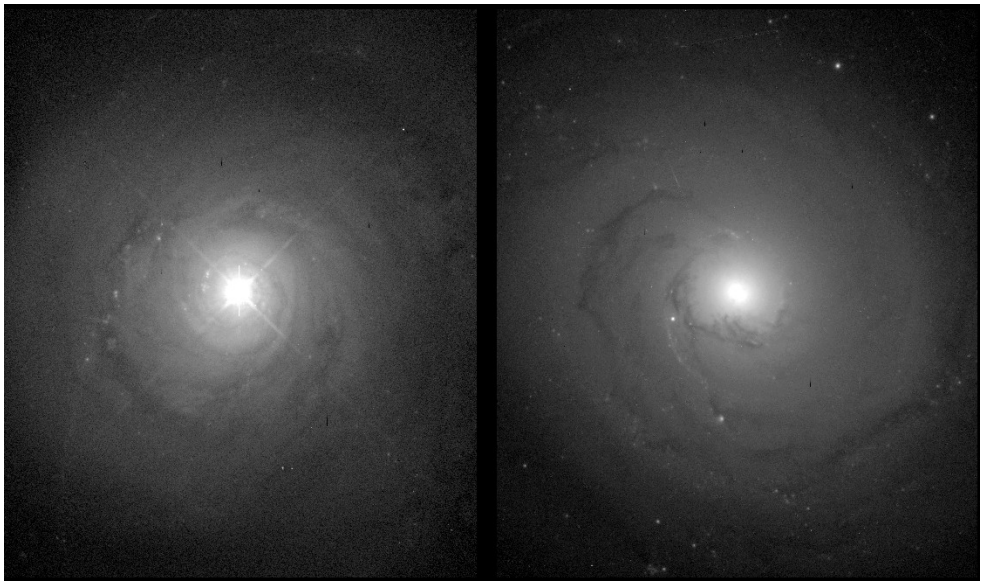

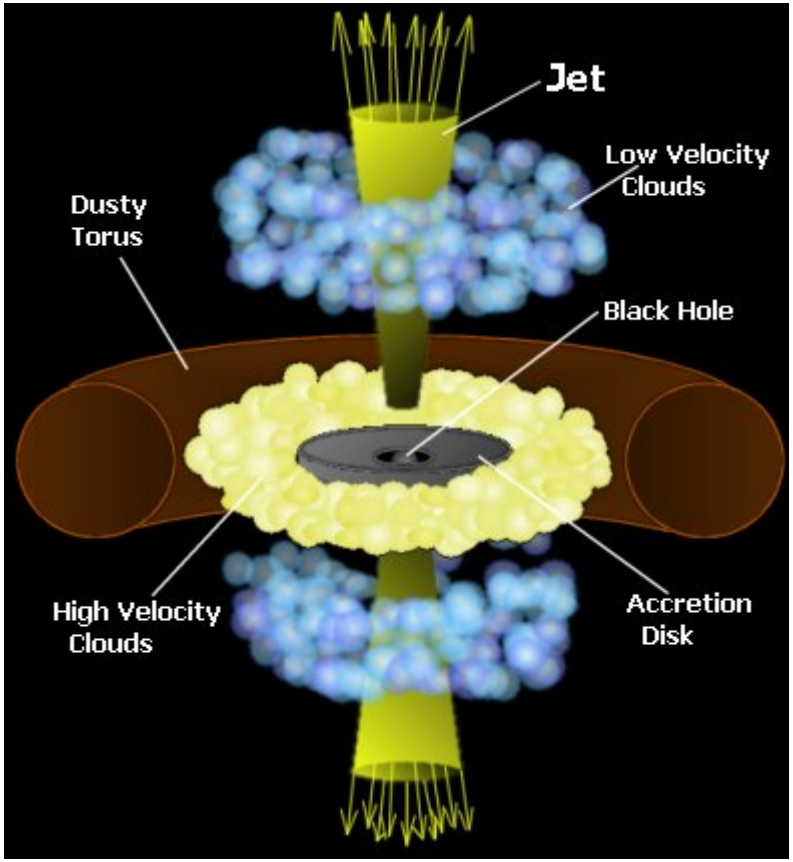

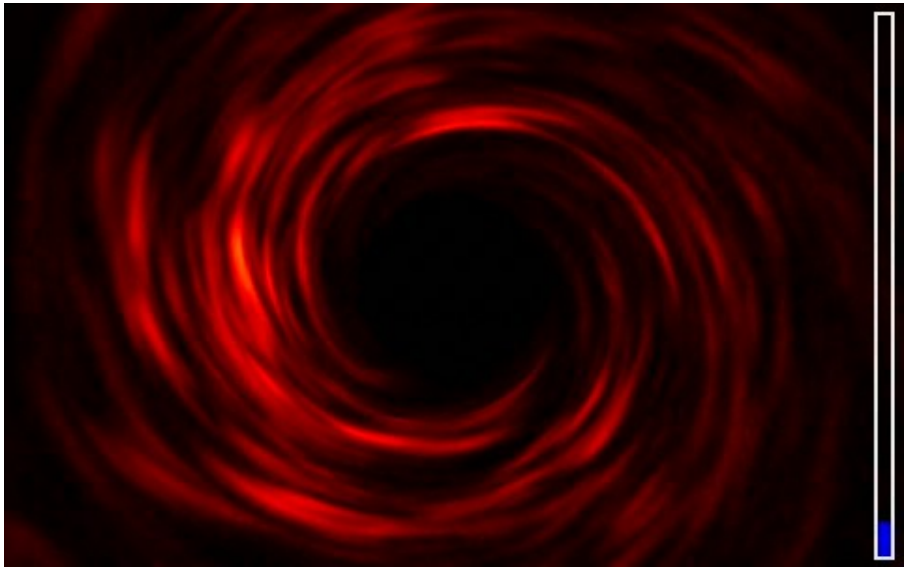

Broad Fe Kα spectral line emitted from relativistic accretion disk

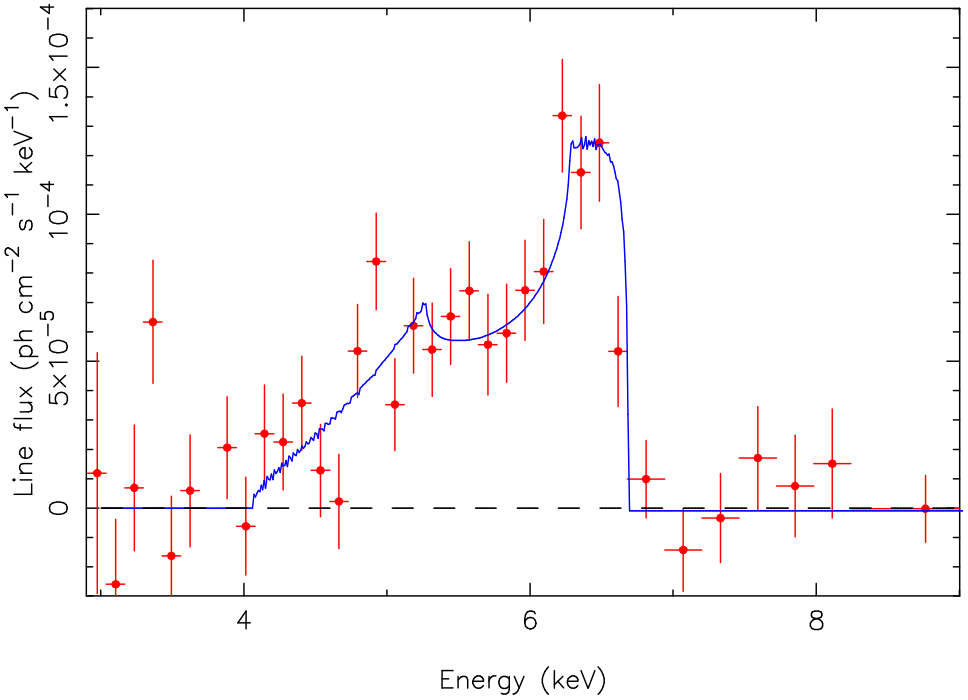

The Fe Kα line profile from Seyfert I galaxy MCG-6-30-15 observed by the ASCA (Tanaka, Y. et al, 1995, *Nature,* **375**, 659) and the modeled profile expected from an accretion disk around a Schwarzschild BH.

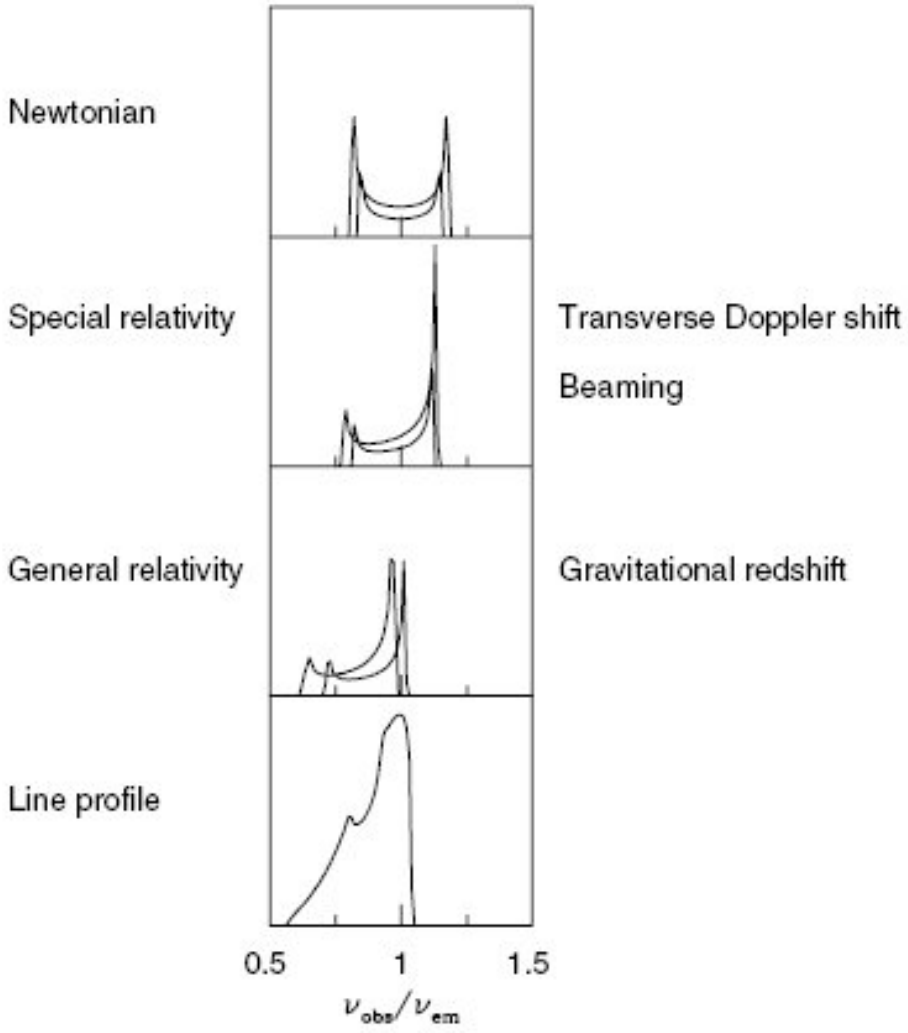

Simulations of radiation from relativistic accretion disk based on ray-tracing in Kerr metric

- Power law surface emissivity of the disk: $\varepsilon(r) = \varepsilon_0 \cdot r^q$
- Photon energy shift: $g = \dfrac{\nu_{obs}}{\nu_{em}}$
- Total observed flux:

$$F_{obs}(E_{obs}) = \int_{image} \varepsilon(r) \cdot g^4 \delta(E_{obs} - gE_0) d\Xi$$

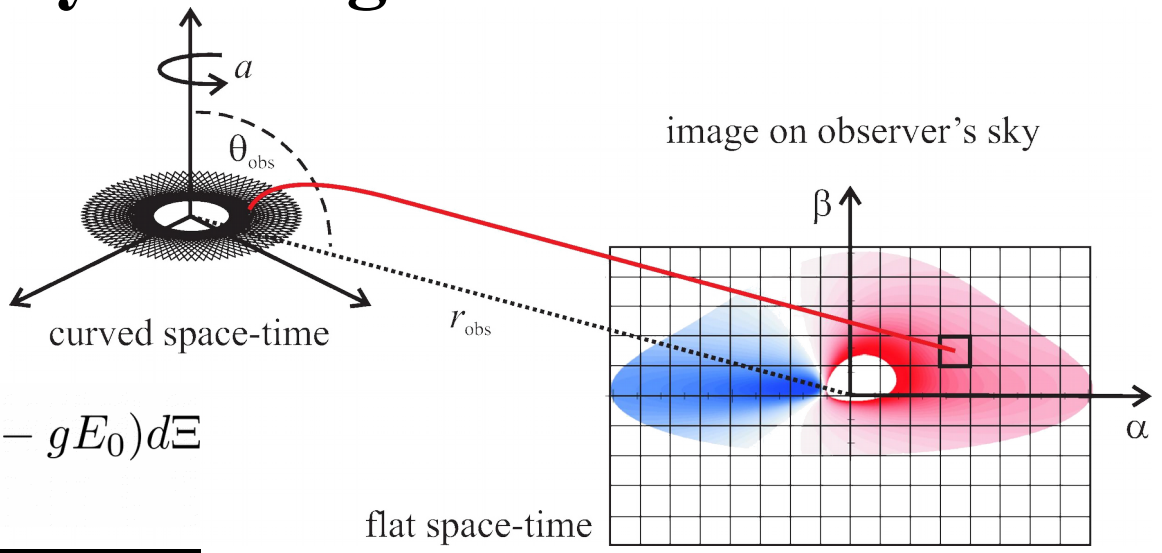

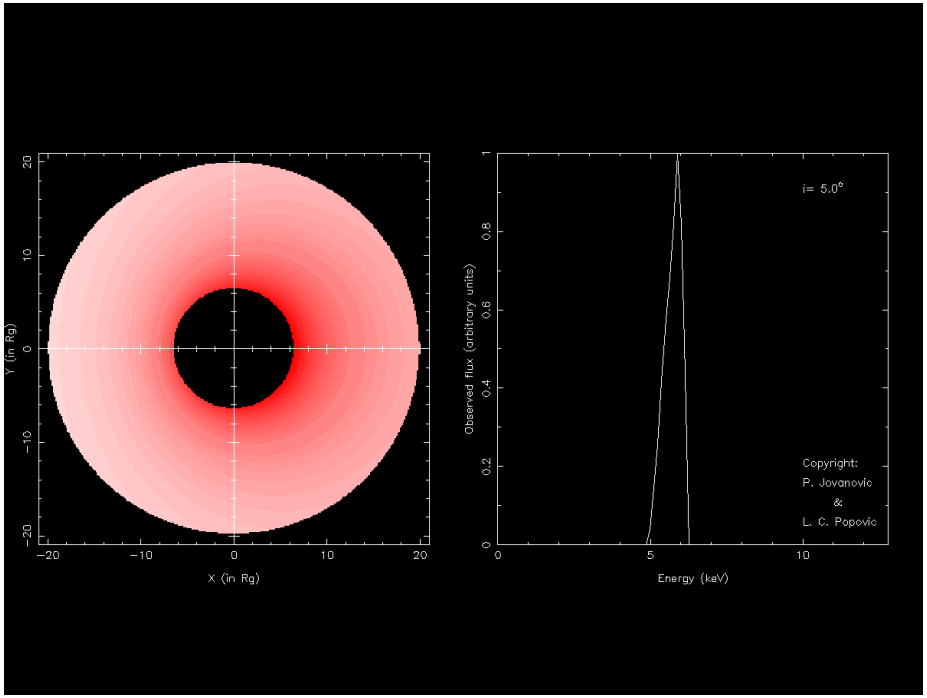

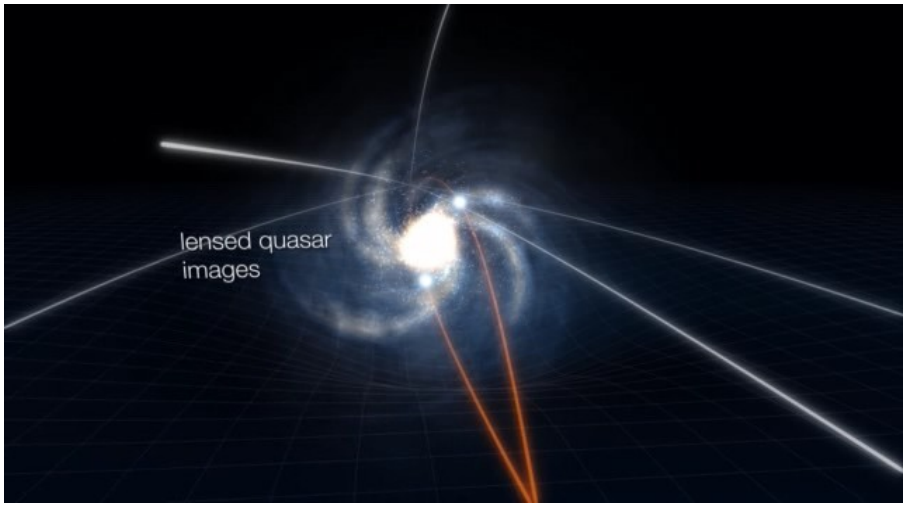

- Applications of gravitational micro-lensing for studying the physics and geometry in vicinity of SMBHs

Point-like microlens

- Amplification due to a single compact object:

$$A(X,Y) = \frac{u^2(X,Y)+2}{u(X,Y)\sqrt{u^2(X,Y)+4}}, \quad u(X,Y) = \frac{\sqrt{(X-X_0)^2+(Y-Y_0)^2}}{\eta_0}$$

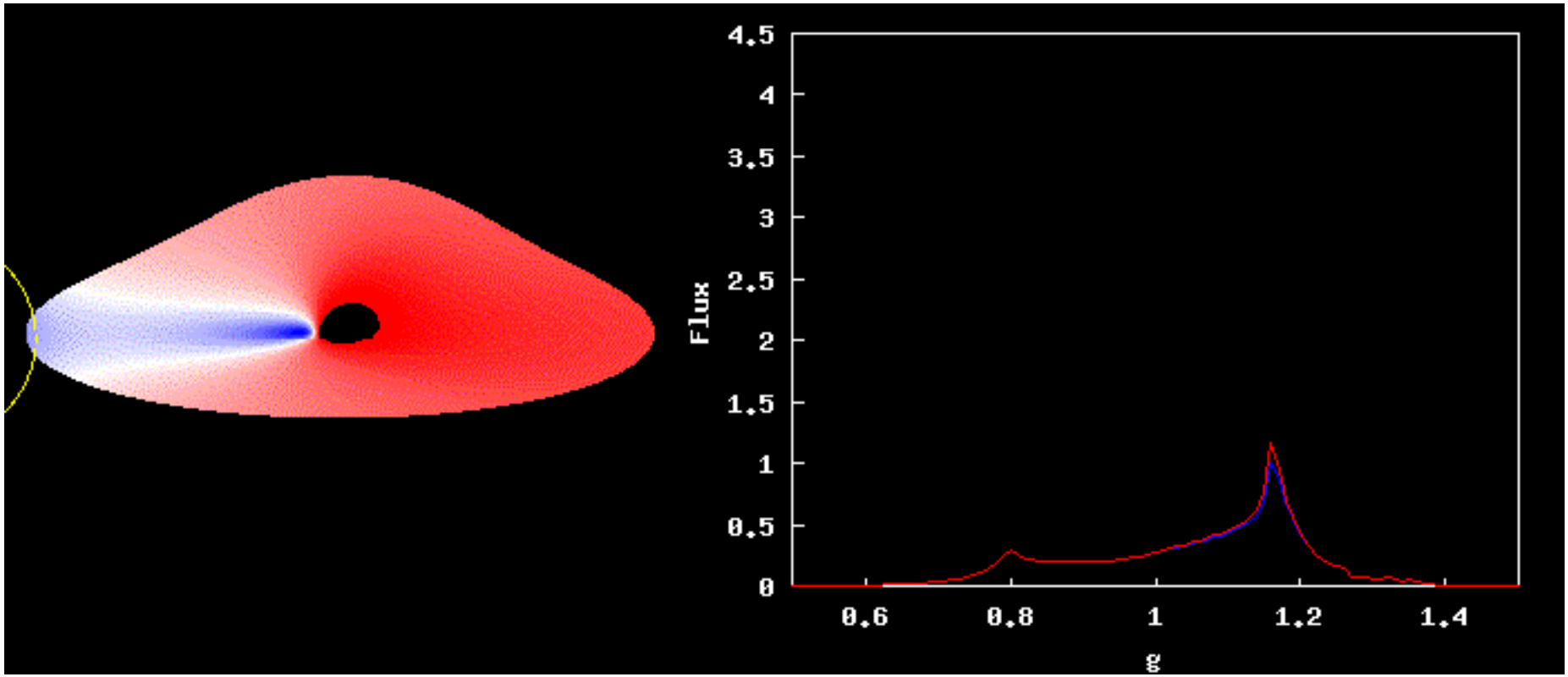

Influence of a point-like microlens on X-ray radiation from a relativistic accretion disk around a SMBH

Straight-fold caustic

- Amplification due to a group of compact objects which projected Einstein radius is larger than accretion disk: $A(X,Y) = A_0 + \frac{K}{\sqrt{\kappa(\xi - \xi_c)}} \cdot H(\kappa(\xi - \xi_c)), \quad K = A_0 \beta \sqrt{\eta_0}$
- Heaviside function: $H(\kappa(\xi - \xi_c)) = 1$ for $\kappa(\xi - \xi_c) > 0$, otherwise it is equal to 0

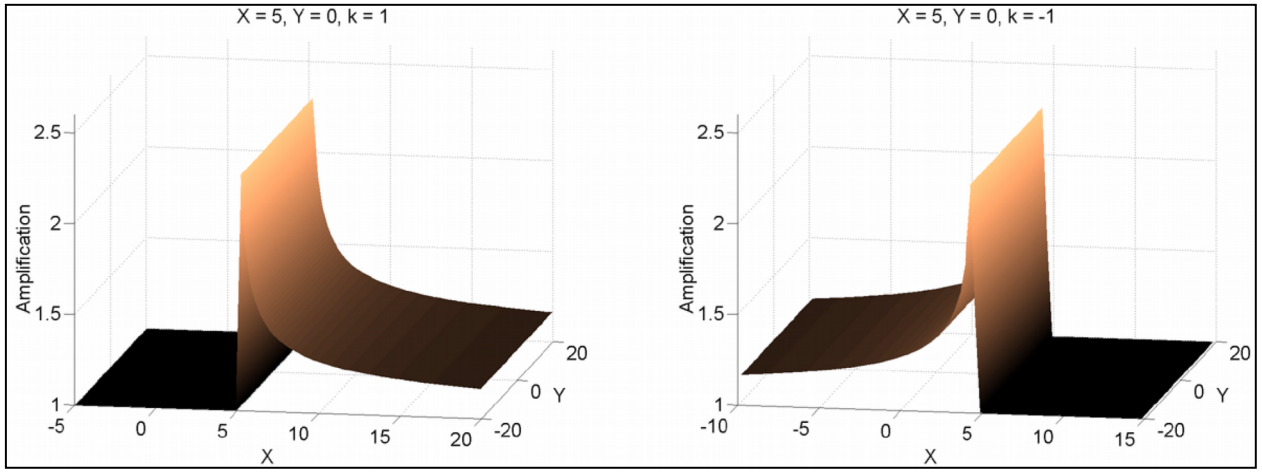

Influence of a straight-fold caustic on X-ray radiation from a relativistic accretion disk around a SMBH

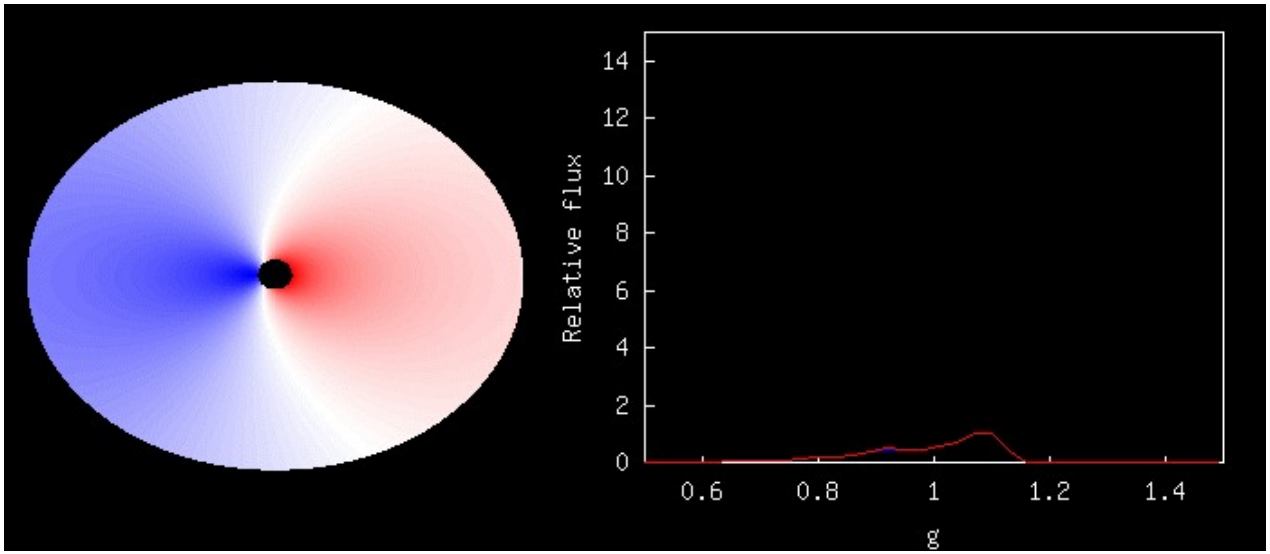

Quadruple microlens

- Lens equation: $\vec{y} = \sum_{1=1}^{N} m_i \frac{\vec{x} - \vec{x}_i}{|\vec{x} - \vec{x}_i|^2} + \begin{bmatrix} 1 - \kappa_c + \gamma & 0 \\ 0 & 1 - \kappa_c - \gamma \end{bmatrix} \vec{x}$

  N - number of microlenses, m_i - their masses, $\vec{x}_i$ - their positions, κ_c - a smooth surface mass density, γ - an external shear (the sum describes the light deflection by the stars and the second term is a quadruple contribution from the galaxy containing the stars)
- A spatial distribution of magnifications in the source plane, due to a random star field in the lens plane: **microlensing magnification map (pattern) or caustic network**
- The most realistic microlens model
- **Inverse/backwards ray shooting**: a large number of light rays is shot from the observer through the randomly generated microlens field in the lens plane, then mapped via the lens equation and collected in the pixels of the source plane

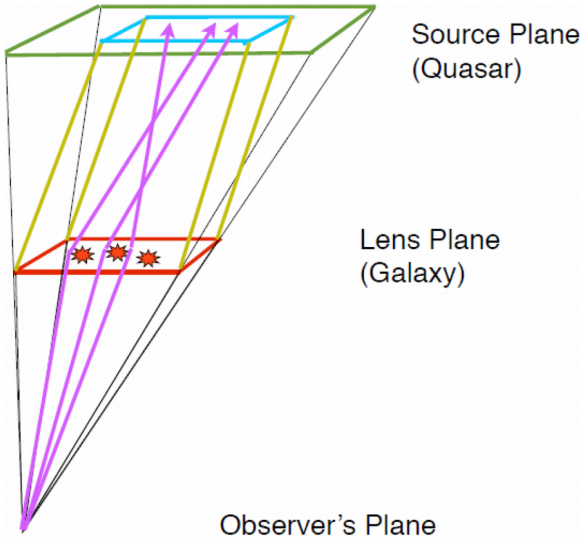

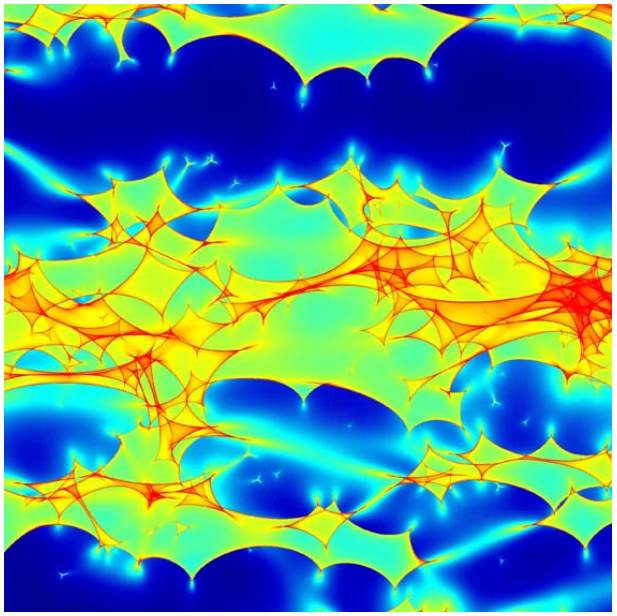

Microlensing magnification map for image A of QSO 2237+0305 ($\kappa_c = 0.36$, $\gamma = 0.4$)

- The number of rays in each pixel is proportional to the magnification factor of a pixel-sized (point-like) source

Microlensing of gravitationally lensed quasars

- different amplifications of X-ray continuum and the Fe Kα line

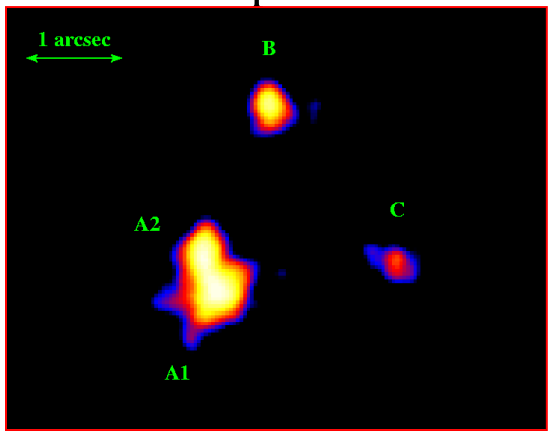

MG J0414+0534

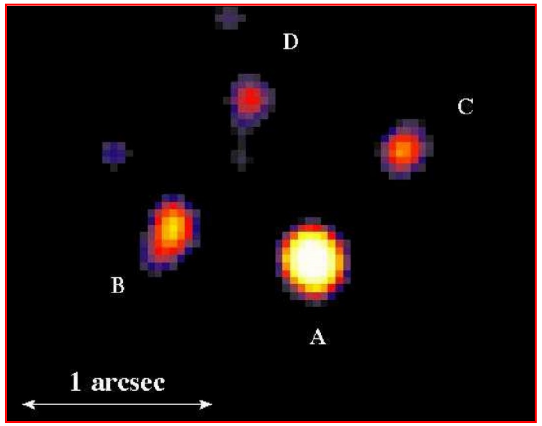

H 1413+117

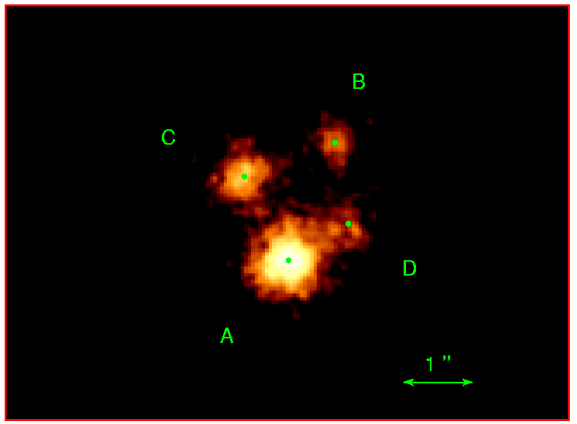

QSO 2237+0305

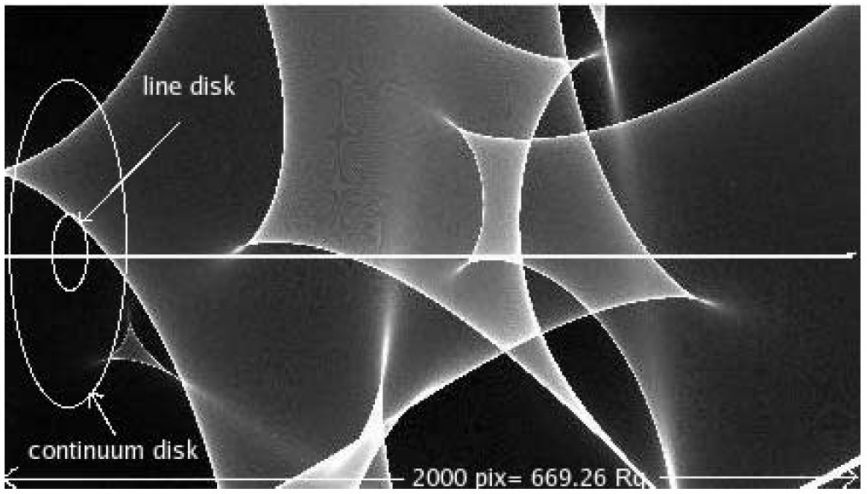

FIG. 9.—Microlensing map of QSO 2237+0305A image with 1 ERR × 2 ERR (1000 pixel × 2000 pixel = $334.63R_g \times 669.26R_g$) on a side and scheme of the projected disk with outer radius $R_{\rm out} = 20R_g$ and $100R_g$ for the Fe Kα line and the X-ray continuum, respectively. The straight line presents the path of the center of the disk (the left side of the pattern corresponds to 0 pixels).

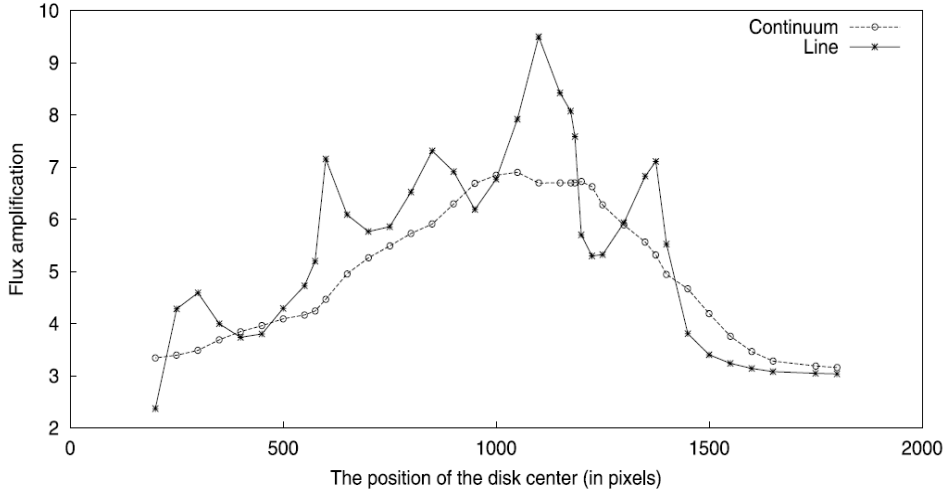

FIG. 10.—Amplification of the Fe Kα line and the X-ray continuum total flux for different positions of the center on the microlensing map of QSO 2237+0305A image (see Fig. 9).

Flux anomaly due to gravitational microlensing

- optical, UV & X-ray flux ratio anomalies
- wavelength dependent amplification due to microlensing by stars
- differential extinction

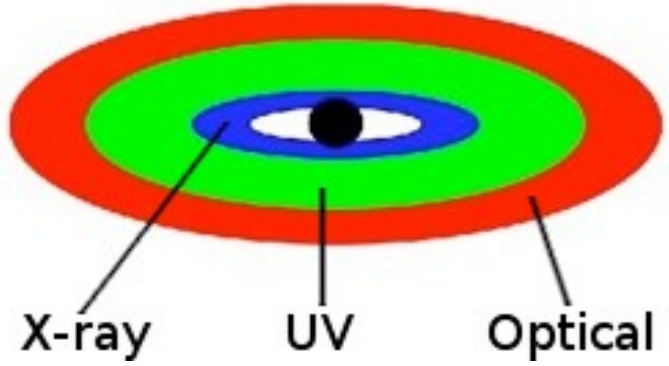

Emitting regions in accretion disk

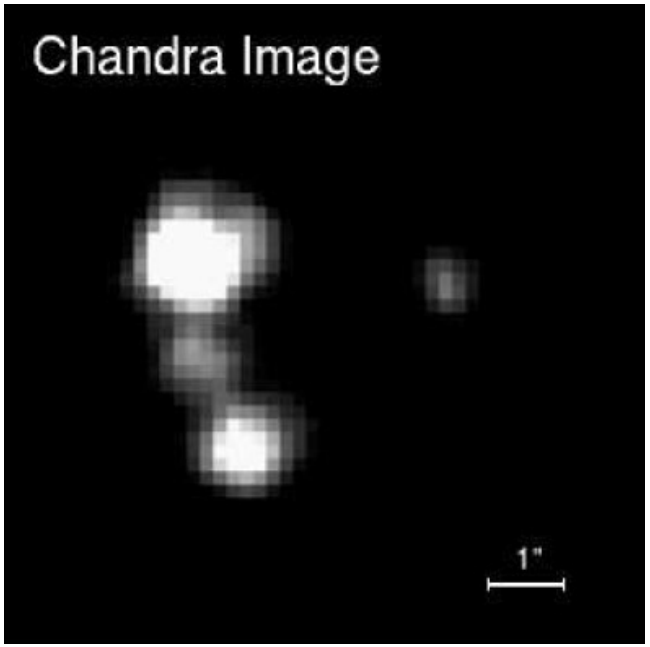

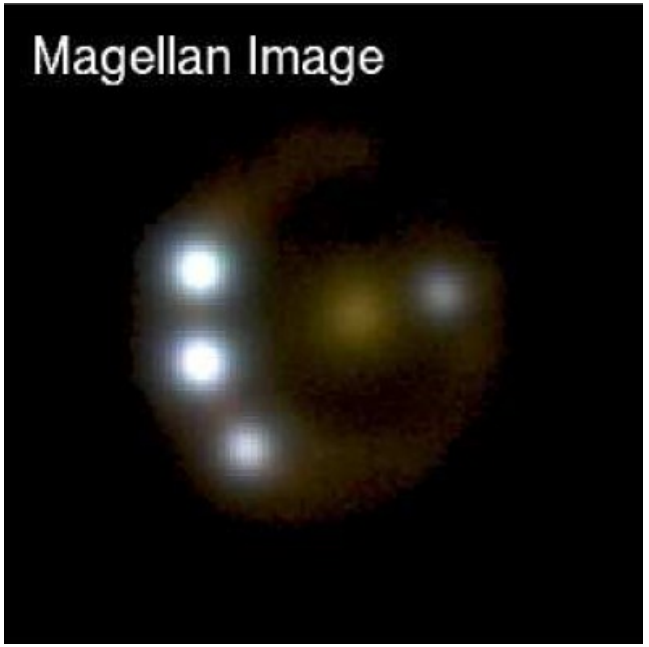

Chandra (*X-ray*) and Magellan (*optical*) images of 1RX J1131-1231

Chromatic effects of gravitational microlensing

- Gravitational lensing is by its nature an achromatic effect

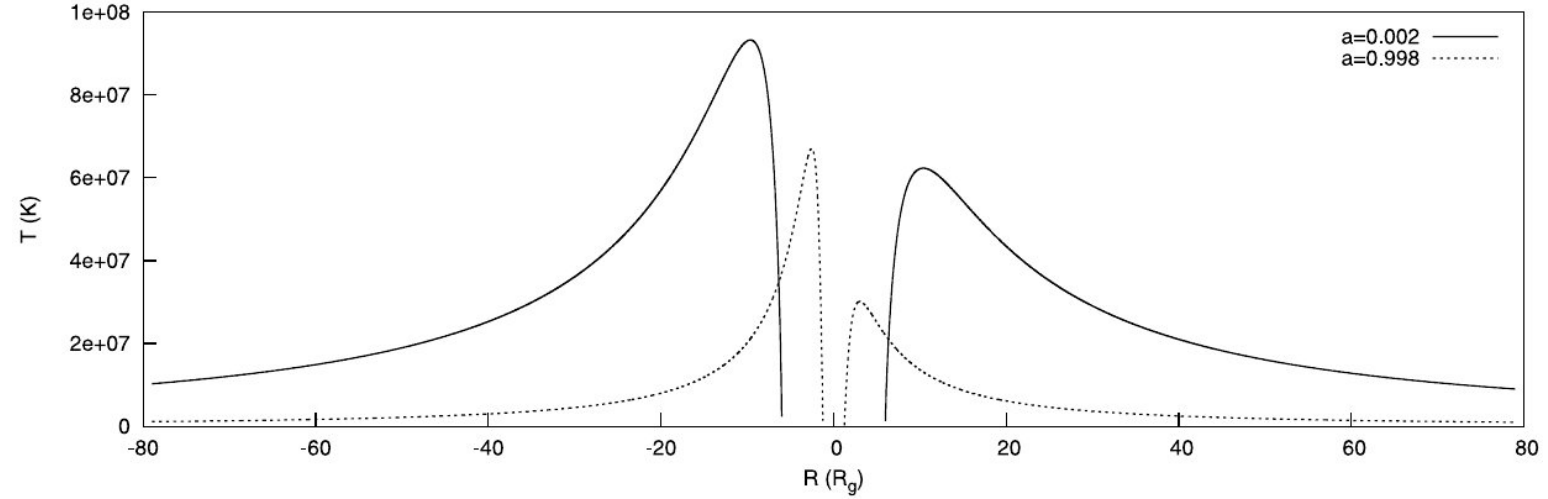

Radial distribution of the temperature along accretion disk

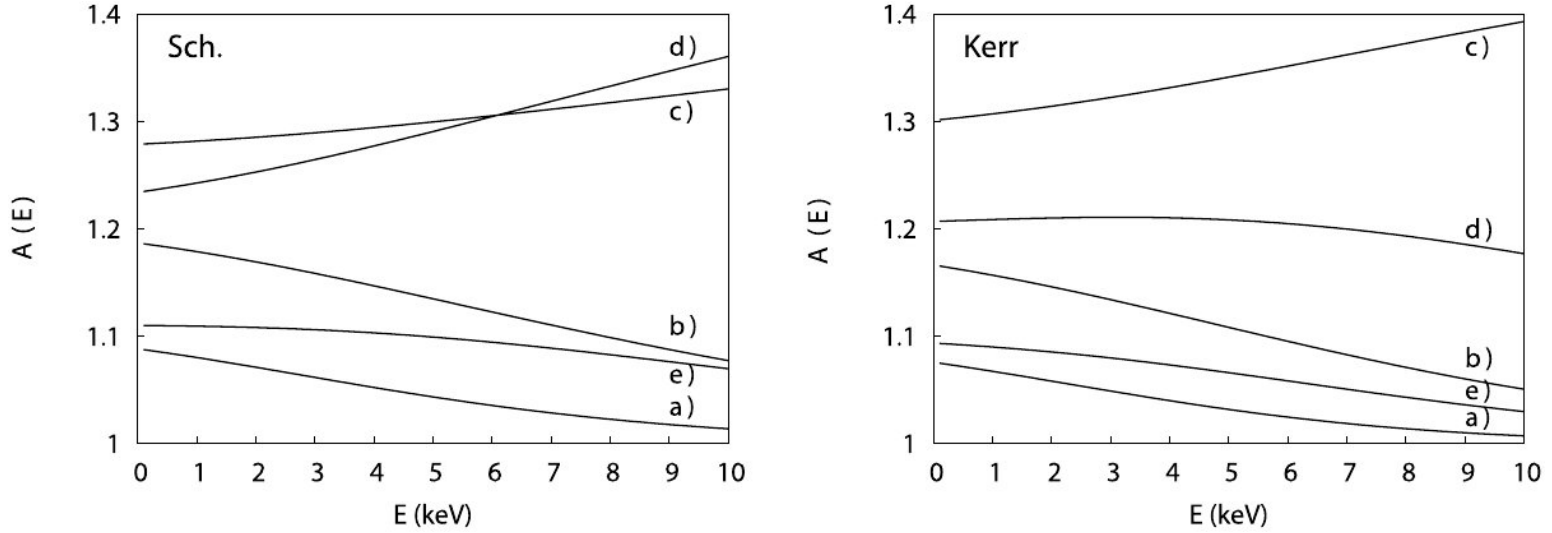

Microlensing amplification of the X-ray continuum as a function of emitted energies (the chromatic effect of microlensing)

Microlensing timescales I

- **The effective source velocity** $v_\perp$ - the velocity of the source relative to the microlens with time measured by the observer (Kayser et al, 1986, A&A, 166, 36):

$$v_\perp = \frac{1}{1+z_d}\frac{D_{ds}}{D_d}v_0 - \frac{1}{1+z_d}\frac{D_s}{D_d}v_d + \frac{1}{1+z_s}v_s,$$

  where v_s is the source velocity measured in the source plane, v_d is the lens velocity measured in the lens plane and v_0 is the transverse velocity of the observer (which usually can be neglected)

- **Standard timescale** t_E: time taken by a small source to cross the projected Einstein radius R_E of a point-like lens (often denoted also as *ERR*):

$$\boxed{t_E = (1+z_d)\frac{R_E}{v_\perp}}$$

- "***caustic time***" - the time when the source is located in the area near the caustic:

$$t_{caustic} = (1+z_l)\frac{r_{caustic}}{v_\perp(D_s/D_l)}$$

- In the case when source radius R_{source} is larger or at least close to the "caustic size" r_{caustic}, the relevant timescale is the "***crossing time***":

$$t_{cross} = (1+z_l)\frac{R_{source}}{v_\perp(D_s/D_l)}$$

Microlensing timescales II

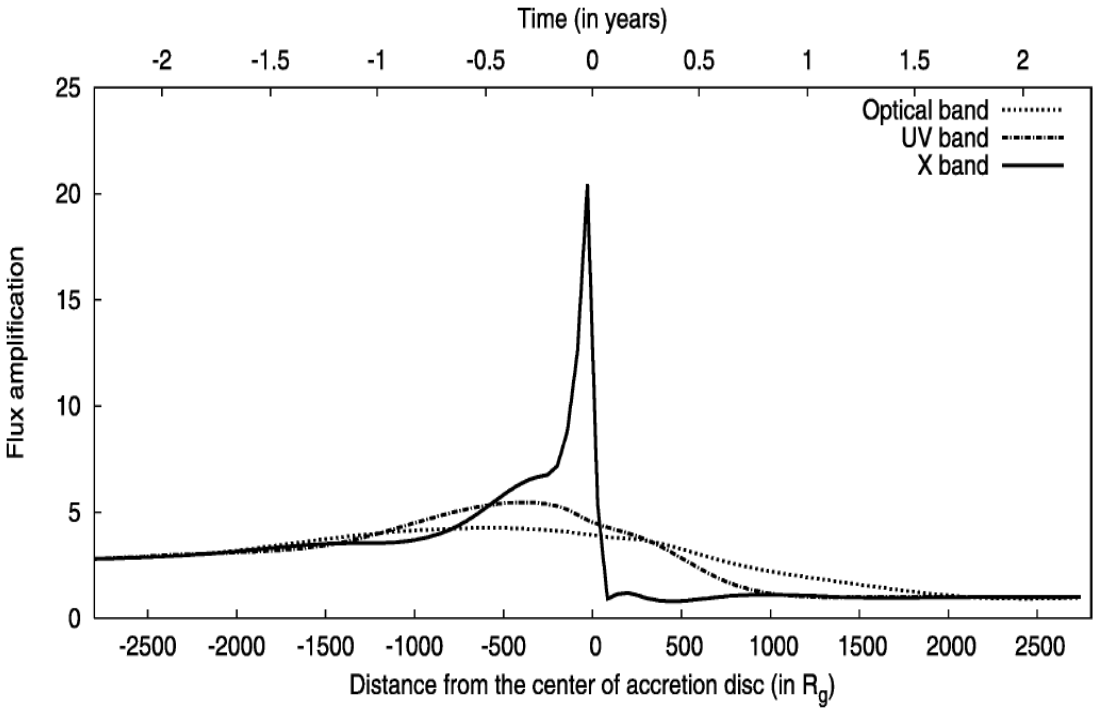

Object	z_s	z_l	X-ray		UV		Optical	
			$t_{caustic}$	t_{HME}	$t_{caustic}$	t_{HME}	$t_{caustic}$	t_{HME}
HS 0818+1227	3.115	0.39	0.572	0.660	7.147	7.070	14.293	15.160
RXJ 0911.4+0551	2.800	0.77	0.976	1.120	12.200	12.080	24.399	25.880
LBQS 1009−0252	2.740	0.88	1.077	1.240	13.468	13.330	26.935	28.570
HE 1104−1805	2.303	0.73	0.918	1.050	11.479	11.370	22.957	24.350
PG 1115+080	1.720	0.31	0.451	0.520	5.634	5.570	11.269	11.950
HE 2149−2745	2.033	0.50	0.675	0.780	8.436	8.350	16.871	17.890
Q 2237+0305	1.695	0.04	0.066	0.080	0.828	0.820	1.655	1.760

Simulated light curves

- Magnification as a function of time during relative motion of a source along some path on microlensing map

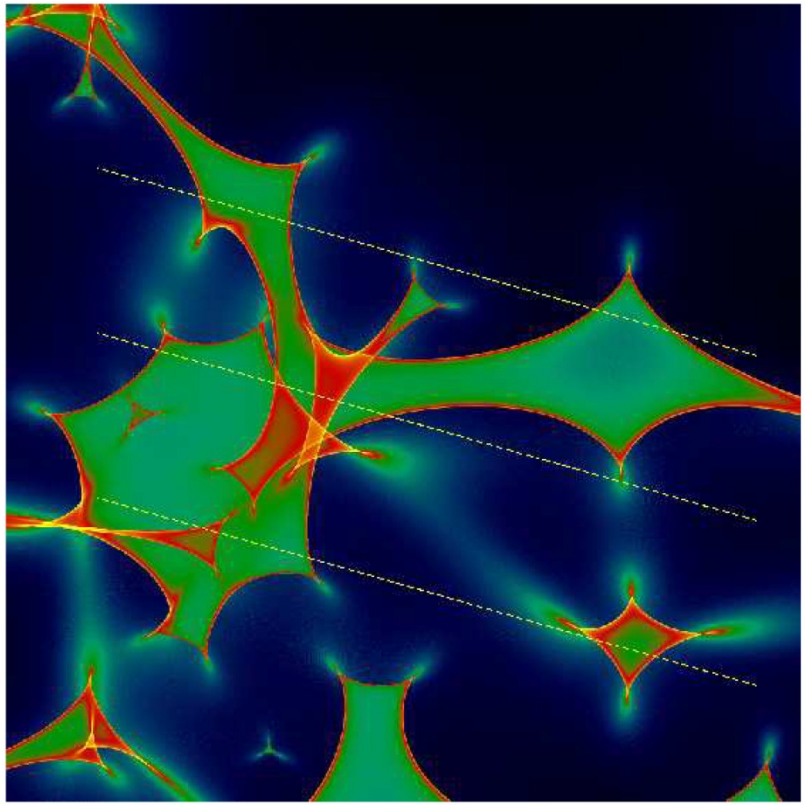

Fig. 44. Microlensing magnification pattern produced by stars in a lensing galaxy. The color steps represent different magnifications, with the sharp caustic lines corresponding to the highest magnification. The dashed lines indicates three tracks along which a background quasar moves. The corresponding lightcurves are displayed in Fig. 45

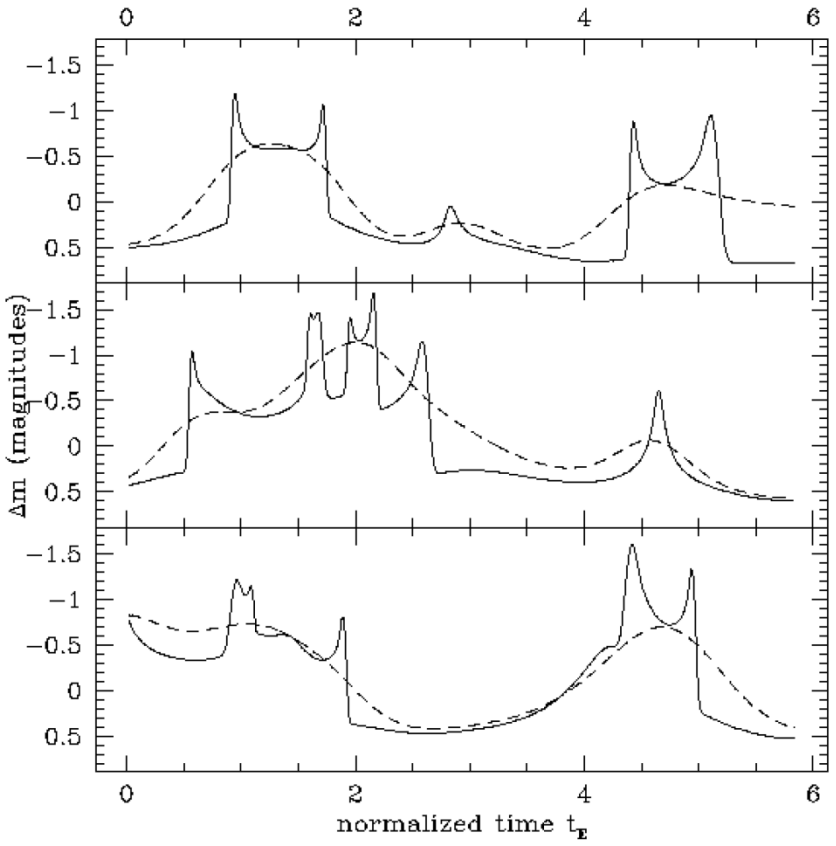

Fig. 45. Microlensing lightcurves for the three tracks shown in Fig. 44. The solid line correspond to a small source (Gaussian shape with width of about 3% of the Einstein radius), the dashed line represents a source that is a factor of 10 larger

Microlensing of extended sources

- For an extended source, its profile must be convolved with the magnification map to find its magnification due to microlensing at each location in the source plane

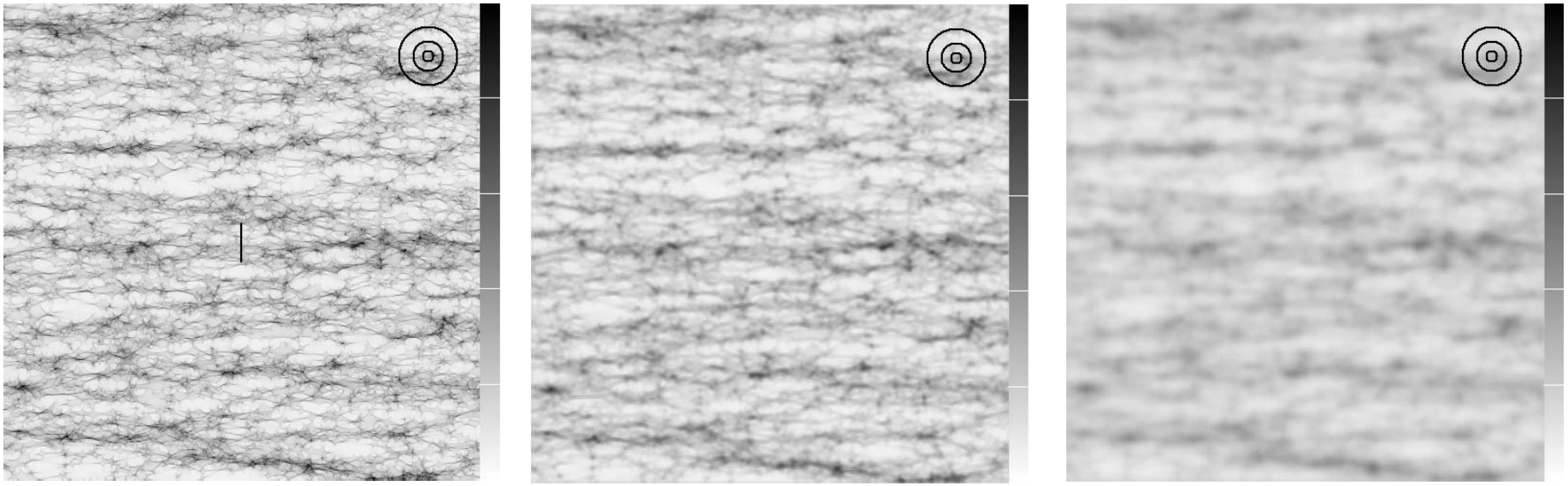

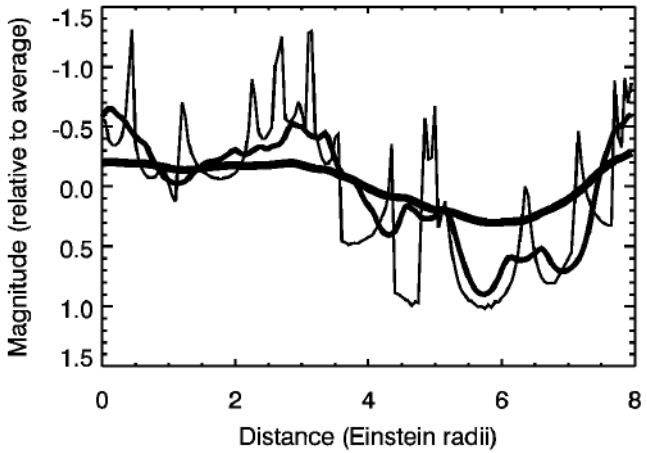

Top: magnification maps of 100 ERR x 100 ERR in the source plane for an image with $\kappa = \gamma = 0.4$, and for three circular sources with radii of 1, 3, and 6 ERR. **Bottom**: The corresponding simulated light curves for a vertical source path of length 4 ERR in the center of each map (Mortonson et al. 2005, ApJ, 628, 594)

Simulated light curves of X-ray, UV and optical radiation from AGN

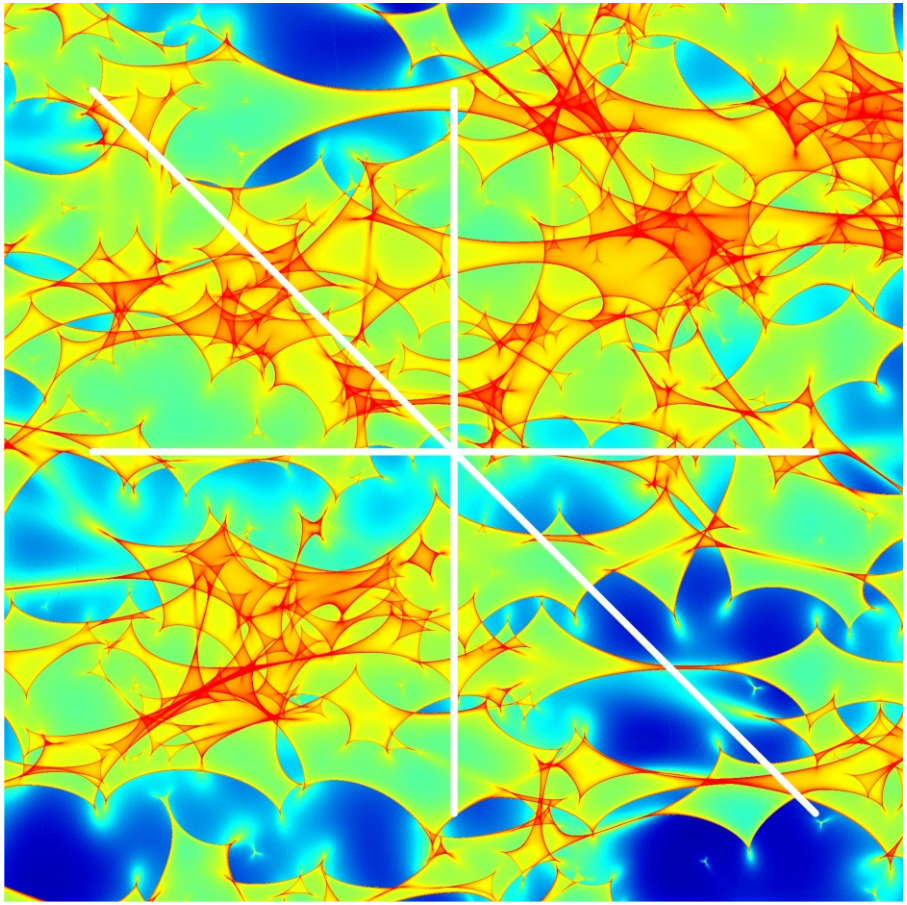

Magnification map of a "typical" lens system, where the white solid lines represent three analyzed paths of an accretion disk.

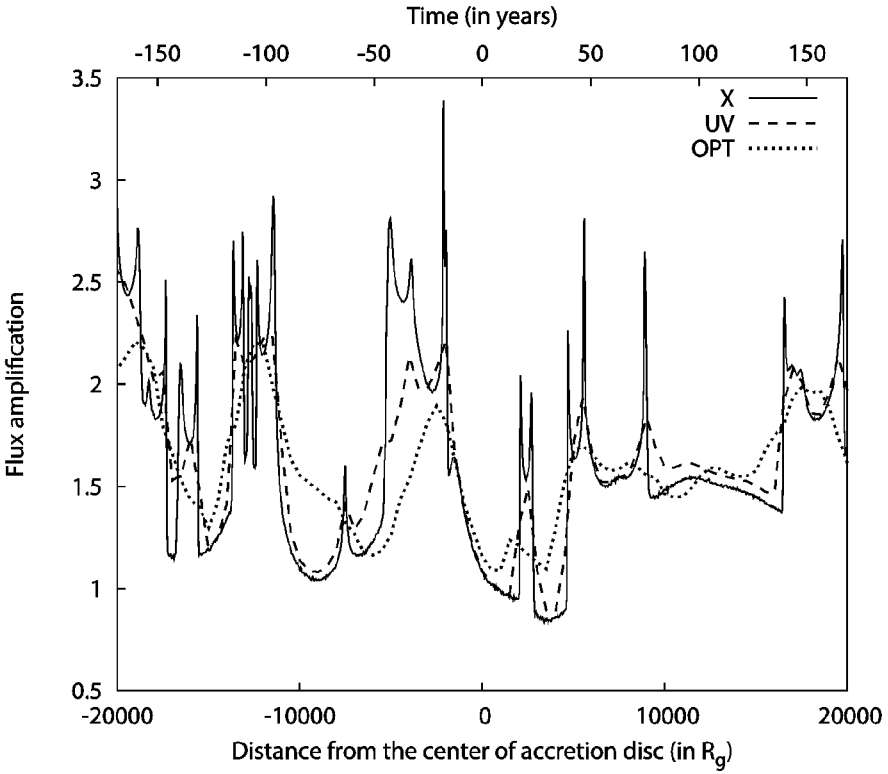

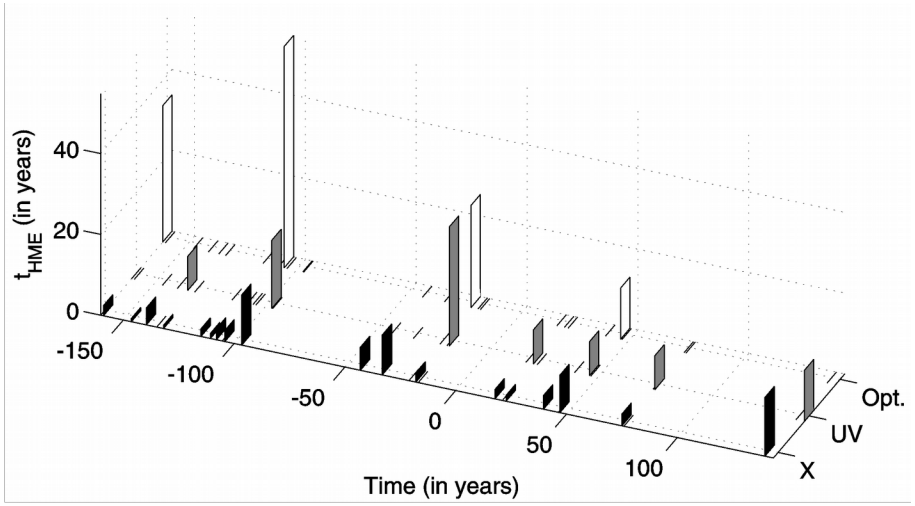

Optical depth and statistics of strong lenses

- **Optical depth (τ)** - the probability of a source being lensed
- τ - the chance of seeing a lensing event, i.e. the probability that at any instant of time a source is within the Einstein ring of a lens
- **Cross section of strong lensing (A)** - area in the lens plane where the separation between the lens and source is sufficiently small for strong lensing to occur (fraction of the sky in which you can place a source and see the lensing effect): $A = \pi\theta_E^2$
- Differential optical depth per unit redshift: $\frac{d\tau}{dz_l} = n(\Delta\theta, z_l)(1+z_l)^3 A \frac{c\,dt}{dz_l}$, where $n(\Delta\theta, z_l)$ is the comoving number density of lenses at z_l producing an image separation $\Delta\theta$, and cdt/dz_l is the proper distance interval
- The total τ is obtained by summing the cross sections of all deflectors between observer and source, or equivalently by: $\tau = \int_0^{z_s} \frac{d\tau}{dz_l} dz_l$
- $\tau \Rightarrow$ several **statistical distributions**: $d\tau/d\Delta\theta$ - describes the distribution of image separations, $d\tau/dz_l$ - gives the redshift distribution of lens galaxies, $d^2\tau/(dz_l\, d\Delta\theta)$ - gives the joint distribution for both z_l and $\Delta\theta$
- **Relative probability** of finding a lens at some z_l: $\delta p_l = \frac{d\tau}{dz_l}/\tau$

Optical depth of SIS strong lenses

$$\tau_{SIS}(z_l, z_s, \Omega_M, \Omega_\Lambda) = \frac{1}{4\pi}\int_0^{z_s} dV \int_0^{\infty} d\sigma \cdot \frac{dn}{d\sigma} \cdot A_{SIS}(\sigma, \Omega_M, \Omega_\Lambda, z_l, z_s),$$ where:

- dV - comoving volume element: $V = \frac{4}{3}D_C^3 \Rightarrow dV = 4D_C^2 \cdot dD_C,\ D_C = D_C(z_l)$
- A_{SIS} - multiple imaging cross section of a SIS lens (angular area between two images): $\theta_E = 4\pi\frac{\sigma^2}{c^2}\frac{D_{ls}}{D_s} \overset{A=\pi\theta_E^2}{\Rightarrow} A_{SIS} = 16\pi^3\left(\frac{\sigma}{c}\right)^4\left(\frac{D_{ls}}{D_s}\right)^2$
- Cross section A_{SIS} is usually also multiplied by the magnification bias $B(S_\nu)$
- B - correction to account for magnification of the lensed sources which are consequently observed to be brighter than the rest of their population
- Lensed sources come from a population with a lower flux than the one at which they are observed (S_ν), and since there are more fainter than brighter sources $\Rightarrow B$ increases the chance of finding a lens
- Fitting a probability distribution from an observed sample of strong lenses by a modeled prediction $\Rightarrow \Omega_M \wedge \Omega_\Lambda$ (the results do not depend on H_0)
- It is essentially a comoving volume cosmological test

Statistics of strong lenses: early results

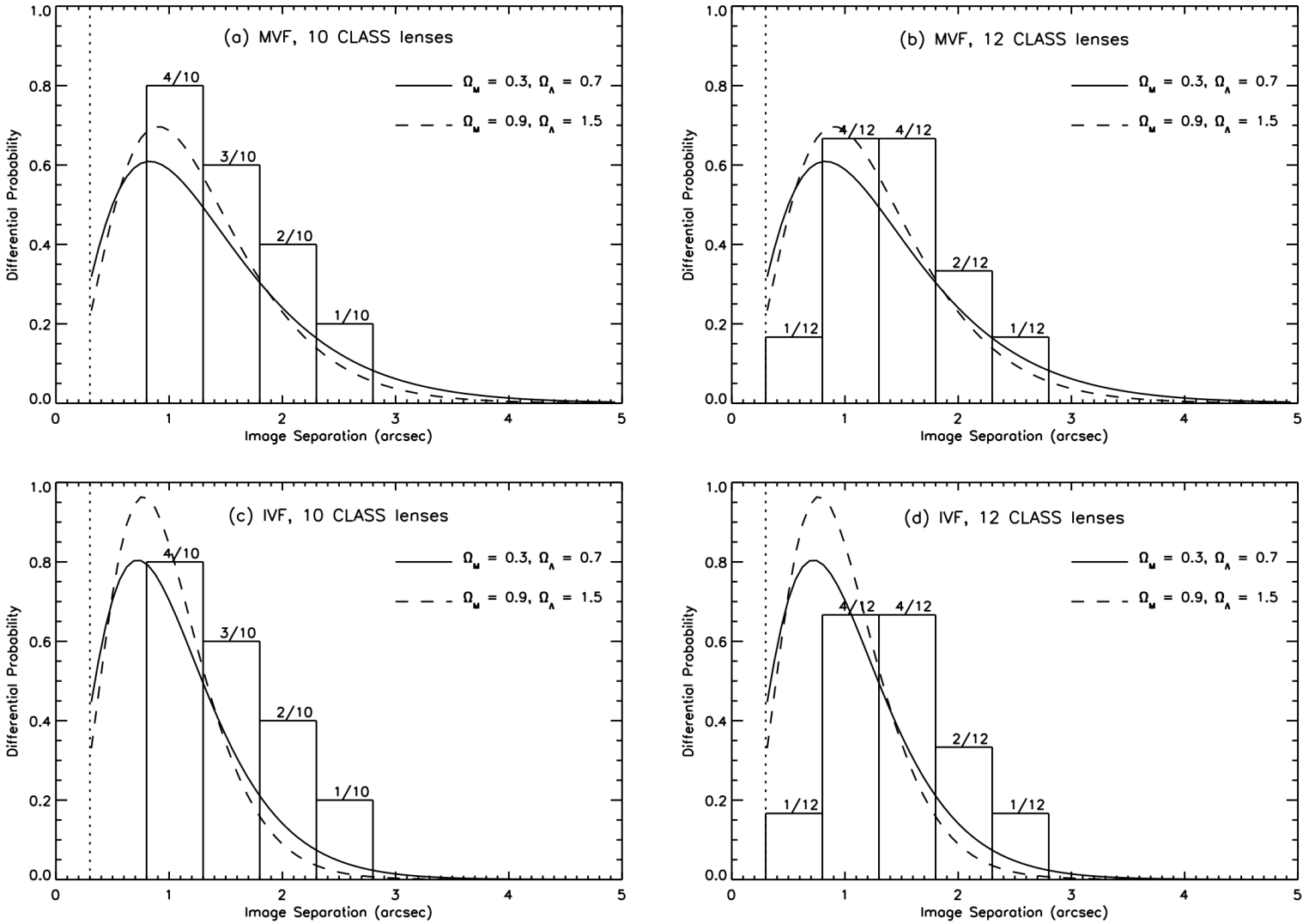

FIG. 6.—Observed CLASS image separation distribution compared to predictions based on the SDSS galaxy sample: (*a*) MVF and 10 lenses, (*b*) MVF and 12 lenses, (*c*) IVF and 10 lenses, (*d*) IVF and 12 lenses. We show model predictions for two different cosmologies: $(\Omega_m,\ \Omega_\Lambda) = (0.3,\ 0.7)$ and $(0.9,\ 1.5)$. The dotted line at $\Delta\theta = 0\farcs3$ indicates the CLASS resolution limit.

(Mitchell et al. 2005, *ApJ*, 622, 81)

Statistics of strong lenses: early results were not in agreement with other cosmological tests

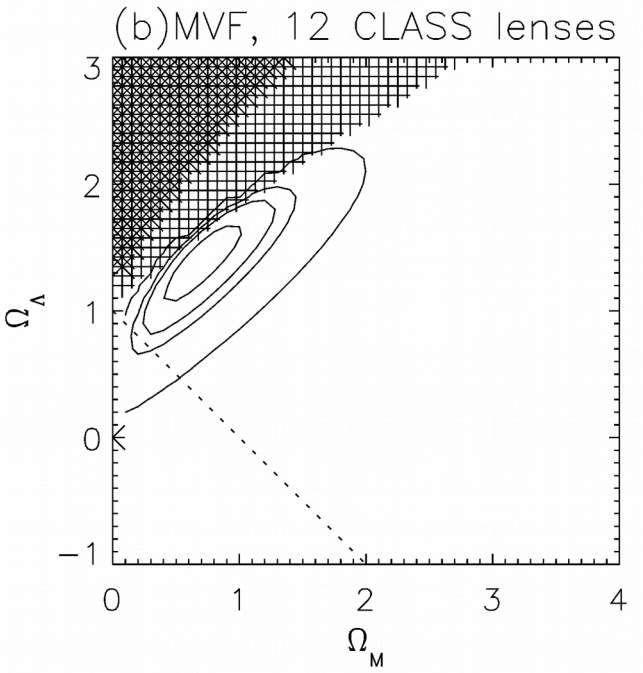

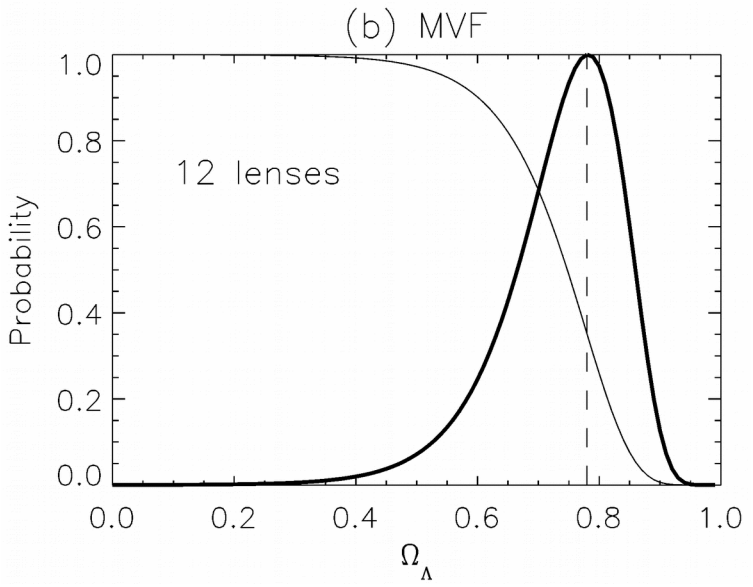

Relative differential probability (thick curve) and cumulative probability (thin curve) for lensing in spatially flat cosmology (Mitchell et al. 2005, *ApJ*, 622, 81)

Impact of Gravitational Lensing on Cosmology
Proceedings IAU Symposium No. 225, 2004
Mellier, Y. & Meylan, G. eds.

doi:10.1017/S1743921305002231

Quasar Lensing Statistics and Ω_Λ: What Went Wrong?

Dan Maoz

Statistics of strong lenses: new results from 2012 in agreement with other cosmological tests

- Cao et al. 2012, *ApJ*, 755, 31
- Oguri et al. 2012, *AJ*, 143 120

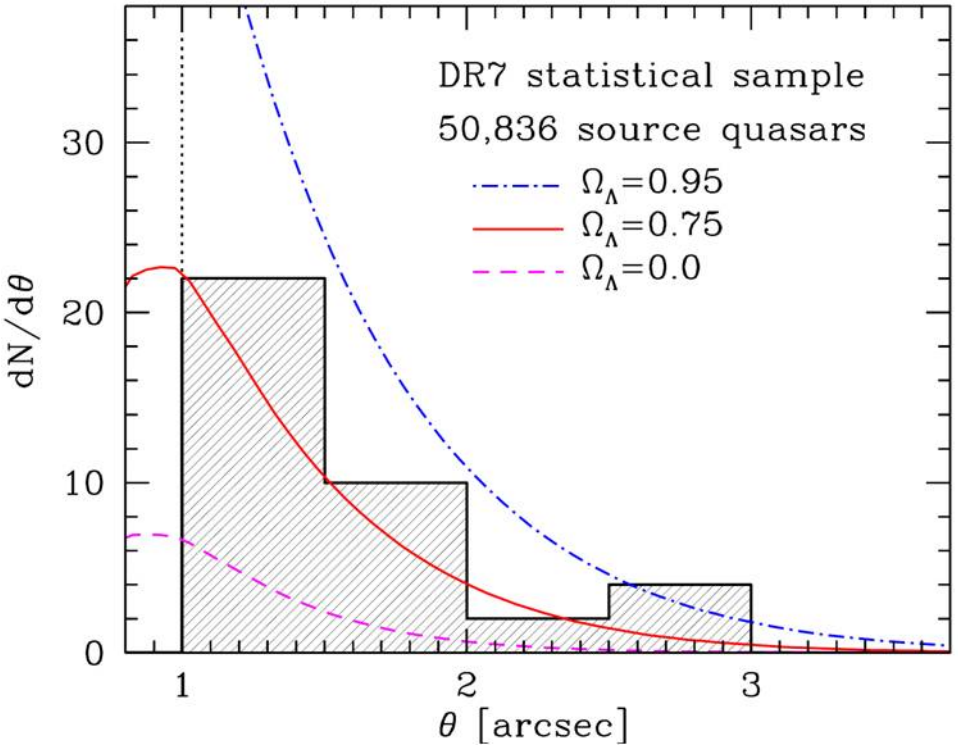

The image separation distribution of the strong lenses in the statistical lens sample

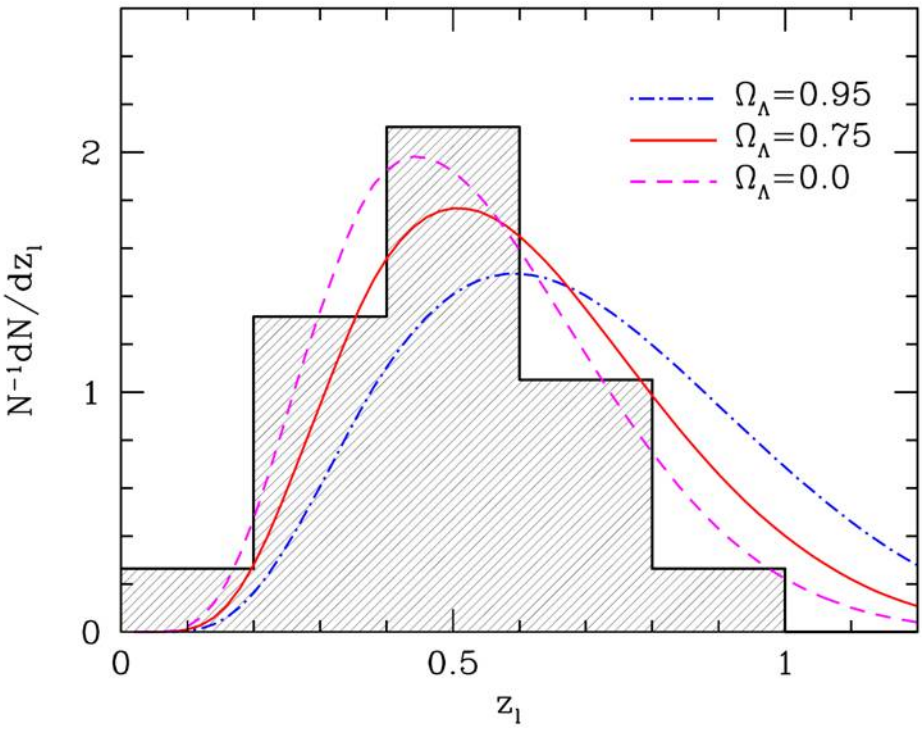

The normalized lens redshift distribution in the sample

Constraints on the cosmological parameters

Left: 1σ and 2σ confidence regions for Ω_M and Ω_Λ for the non-flat models with a cosmological constant

Right: 1σ and 2σ confidence regions for Ω_M and w for the flat dark energy models

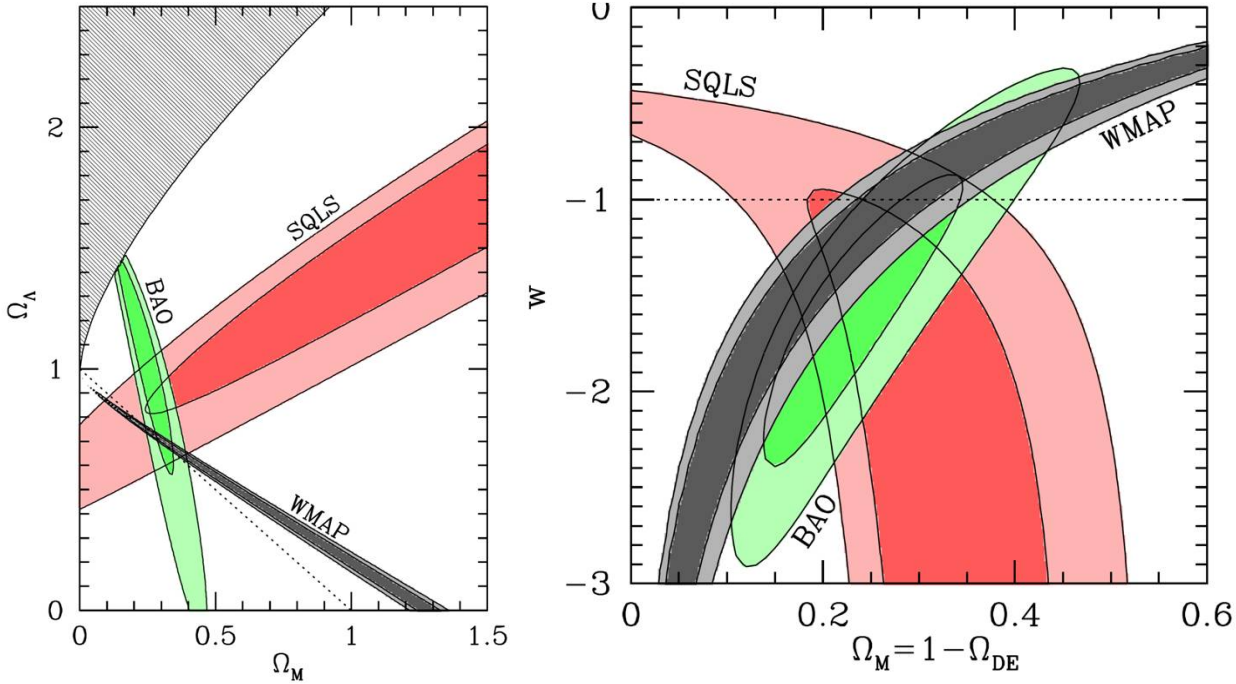

Table 3. Constraints on Cosmological Parameters

Model	Data	Ω_M	$\Omega_{\rm DE}$	w
flat Ω_Λ	SQLS	$\equiv 1-\Omega_\Lambda$	$0.79^{+0.06+0.06}_{-0.07-0.06}$	$\equiv -1$
non-flat Ω_Λ	SQLS+BAO	$0.28^{+0.03+0.02}_{-0.03-0.02}$	$0.88^{+0.09+0.07}_{-0.10-0.09}$	$\equiv -1$
non-flat Ω_Λ	SQLS+WMAP	$0.20^{+0.08+0.07}_{-0.06-0.07}$	$0.78^{+0.05+0.05}_{-0.06-0.05}$	$\equiv -1$
non-flat Ω_Λ	SQLS+BAO+WMAP	$0.29^{+0.02+0.00}_{-0.02-0.00}$	$0.71^{+0.02+0.00}_{-0.02-0.00}$	$\equiv -1$
flat $\Omega_{\rm DE}$	SQLS+BAO	$0.25^{+0.03+0.03}_{-0.03-0.02}$	$\equiv 1-\Omega_M$	$-1.44^{+0.22+0.17}_{-0.25-0.18}$
flat $\Omega_{\rm DE}$	SQLS+WMAP	$0.23^{+0.04+0.03}_{-0.03-0.03}$	$\equiv 1-\Omega_M$	$-1.19^{+0.17+0.14}_{-0.17-0.15}$
flat $\Omega_{\rm DE}$	SQLS+BAO+WMAP	$0.28^{+0.02+0.01}_{-0.02-0.01}$	$\equiv 1-\Omega_M$	$-1.11^{+0.14+0.08}_{-0.17-0.10}$

Optical depth for cosmological distribution of gravitational microlenses

- Ω_L – matter fraction in compact lenses

$$\tau_L^p = \frac{3}{2}\frac{\Omega_L}{\lambda(z)}\int_0^z d\,\omega \frac{(1+\omega)^3[\lambda(z)-\lambda(\omega)]\lambda(\omega)}{\sqrt{\Omega_M(1+\omega)^3+\Omega_\Lambda}}, \qquad \lambda_z = \int_0^z \frac{d\,\omega}{(1+\omega)^2\sqrt{\Omega_M(1+\omega)^3+\Omega_\Lambda}}$$

- $\lambda(z)$ – affine distance (in cH_0^{-1})
- $\Omega_L = 0.01$: 25% of baryonic matter forms microlenses
- $\Omega_L = 0.05$: almost all baryonic matter forms microlenses
- $\Omega_L = 0.1$: about 30% of dark matter forms microlenses

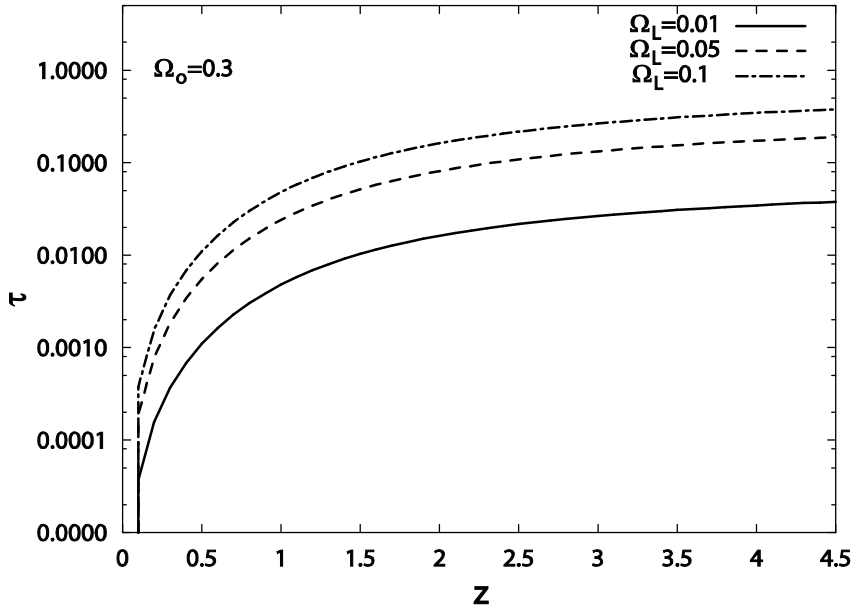

Table 1. The calculated optical depth as a function of redshift for different values of Ω_L and $\Omega_0 = 0.3$.

$z\backslash\Omega_L$	0.01	0.05	0.10
0.5	0.001100	0.005499	0.010998
1.0	0.004793	0.023967	0.047934
1.5	0.010310	0.051550	0.103100
2.0	0.016196	0.080980	0.161959
2.5	0.021667	0.108334	0.216669
3.0	0.026518	0.132590	0.265180
3.5	0.030770	0.153852	0.307703
4.0	0.034504	0.172521	0.345042
4.5	0.037804	0.189018	0.378037
5.0	0.040742	0.203712	0.407424

(Zakharov, Popović & Jovanović, 2004, A&A, 881)

Exam questions

1. Point-like and straight-fold caustic models of gravitational microlenses, their timescales and applications for investigation of physics and space-time geometry in vicinity of supermassive black holes
2. Microlensing magnification map, its influence on extended sources and simulated light curves
3. Optical depth of strong lenses and constraints on the cosmological parameters from their statistics

Literature

Textbook:

- *Gravitational Lensing*: Strong, Weak and Micro, Book Series: Saas-Fee Advanced Courses
  1. P. Schneider - *Introduction to Gravitational Lensing and Cosmology*
  2. C. S. Kochanek - *Strong Gravitational Lensing*
  3. P. Schneider - *Weak Gravitational Lensing*
  4. J. Wambsganss - *Gravitational Microlensing*

Exercise 1

FITS file "disk.fits.gz" contains a simulated image of a highly inclined (i = 75°) relativistic accretion disk which extends between 6 and 30 R_g from the central non-rotating supermassive black hole and emits in the X-ray band according to the power law with emissivity index q = -2.5.

Use the provided Python script to simulate the influence of a point-like microlens with projected Einstein radius $\eta_0 = 5\ R_g$ on the observed profile of the Fe Kα line emitted from the disk. Assume that microlens crosses over the disk along x-axis, from its receding side ($x > 0$) towards its approaching side ($x < 0$), and perform the simulations for the following 5 microlens positions: x = 25, 10, 0, -10, -25 R_g.

Discuss the resulting deformations of the line profile and their dependence on the microlens position.

Exercise 2

Simulate the microlensing light curves due to crossing of a point-like and an extended circular source over the magnification map (given as FITS file "mlmap.fits.gz") for a "typical" lens ($z_d = 0.5$, $z_s = 2$). Assume that both sources cross the map with effective velocity $v_\perp = 5\ R_E$ / yr along its diagonal path between (1 R_E, 1 R_E) and (15 R_E, 15 R_E), and that circular source has radius $R_s = 0.8\ R_E$ and Gaussian distribution of brightness with standard deviation: a) $\sigma = 0.4\ R_E$ and b) $\sigma = 0.1\ R_E$.

Use the provided Python scripts to perform the required simulations, and then discuss the resulting simulated microlensing light curves.

Exercise 3

Calculate the crossing times in the case of a "typical" lens ($z_l = 0.5$, $z_s = 2$) and Einstein Cross ($z_l = 0.04$, $z_s = 1.695$) for a microlens crossing with an effective velocity of $v_\perp = 600$ km/s over a source with 100 AU in size. Assume a flat cosmological model with $H_0 = 75$ km/s/Mpc, $\Omega_M = 0.3$ and $\Omega_\Lambda = 0.7$.

Exercise 4

Optical depth $\tau_{GL}(z_Q)$ of a quasar at a redshift $z_Q = y - 1$ being multiple imaged by a SIS lens along the line of sight can be estimated for $\Omega_\kappa = 0$ by (Turner, 1990, ApJ, 365, L43):

$$\tau_{GL} = \frac{F}{30}\left[\int_1^y \frac{d\,\omega}{\left(\Omega_M\,\omega^3 - \Omega_M + 1\right)^{1/2}}\right]^3, \quad F = 16\,\pi^3\,n_0\left(\frac{c}{H_0}\right)^3\left(\frac{\sigma}{c}\right)^4 \approx 0.15,$$

where F characterizes the lensing effectiveness of a population of SIS lenses with velocity dispersion σ and comoving number density n_0.

a) Plot the optical depth τ_{GL} as a function of z_Q for the following 4 flat cosmological models $\Omega_M = 0.0$, 0.1, 0.3 and 1.0

b) Compare the obtained results with Fig. 1 from Turner, 1990, ApJ, 365, L43

c) What is the value of τ_{GL} for a quasar at $z_Q = 2$ in the case of $\Omega_M = 0.3$?

Solution 1

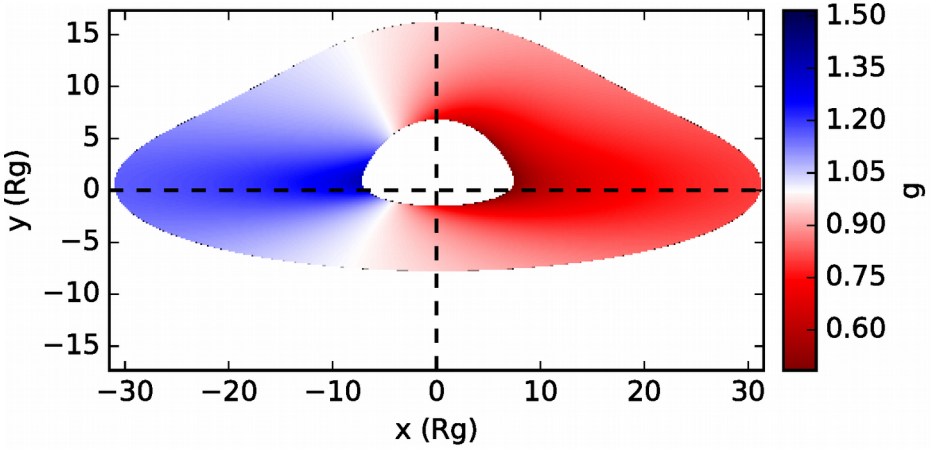

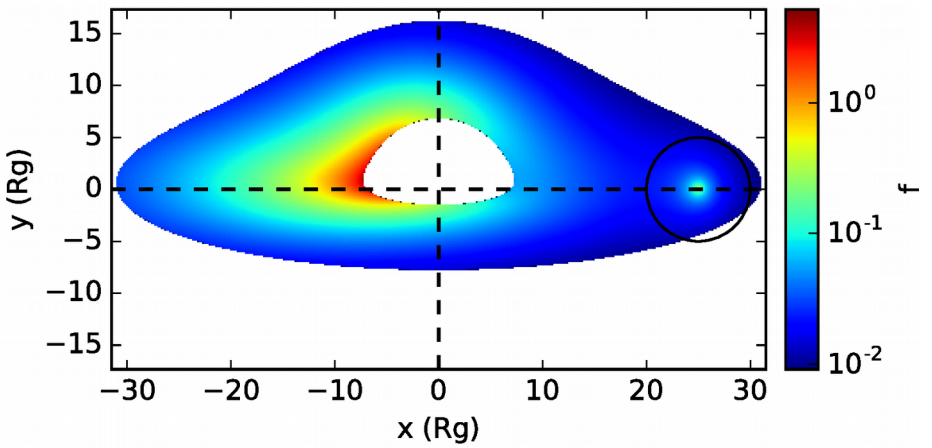

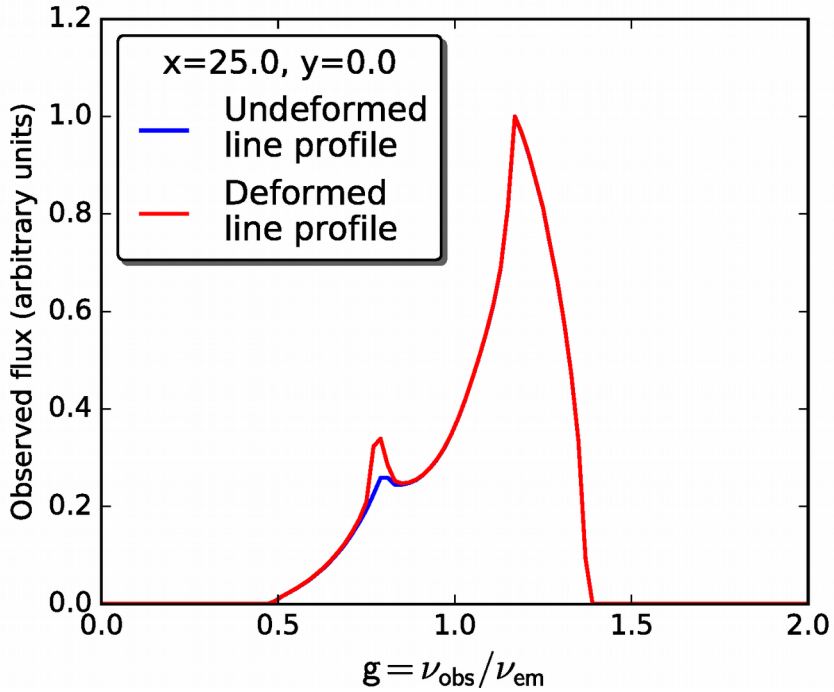

Solution is obtained by the Python script "pointml.py"

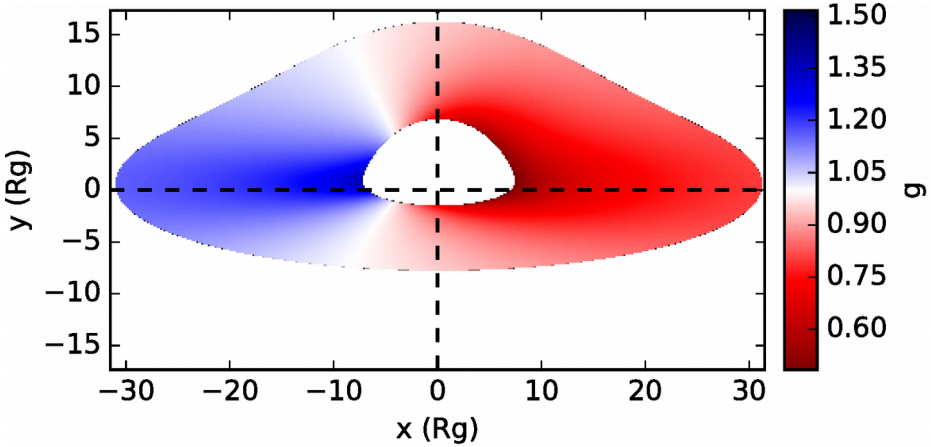
y (Rg)
x (Rg)
g
1.50
1.35
1.20
1.05
0.90
0.75
0.60

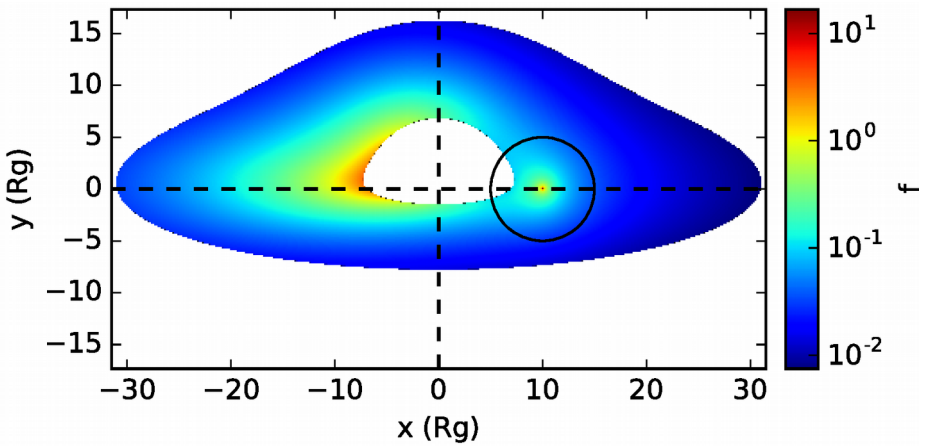
y (Rg)
x (Rg)
f

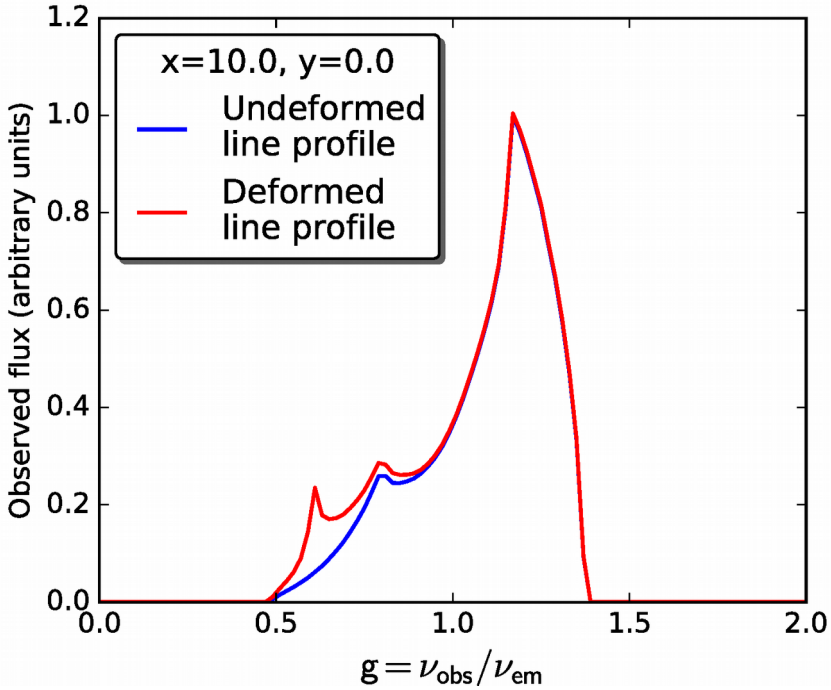
x=10.0, y=0.0
Undeformed line profile
Deformed line profile
Observed flux (arbitrary units)
g = ν_obs / ν_em

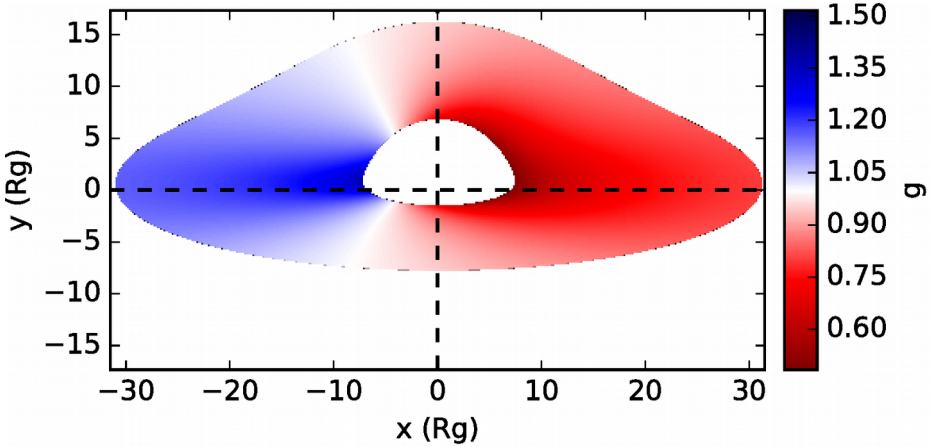
y (Rg)
x (Rg)
g
1.50
1.35
1.20
1.05
0.90
0.75
0.60

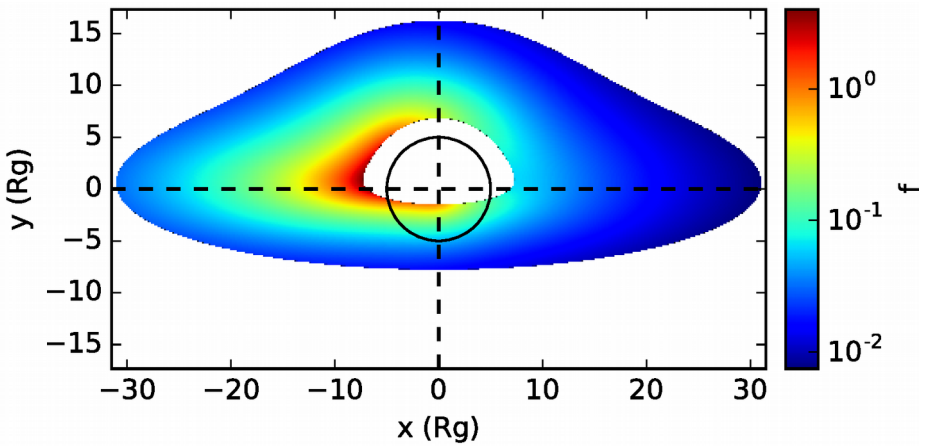
y (Rg)
x (Rg)
f
10^{0}
10^{-1}
10^{-2}

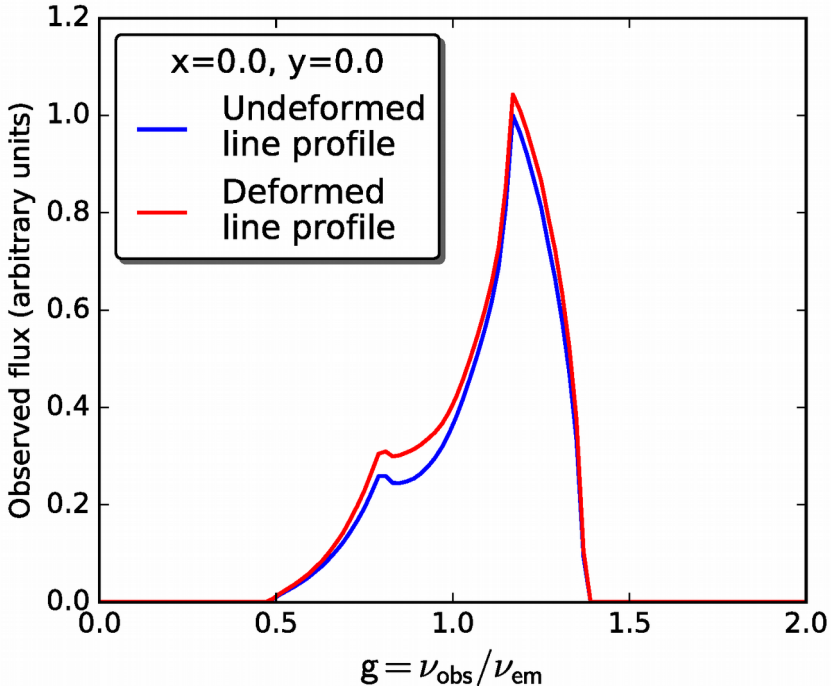
x=0.0, y=0.0
Undeformed line profile
Deformed line profile
Observed flux (arbitrary units)
$g = \nu_{obs}/\nu_{em}$

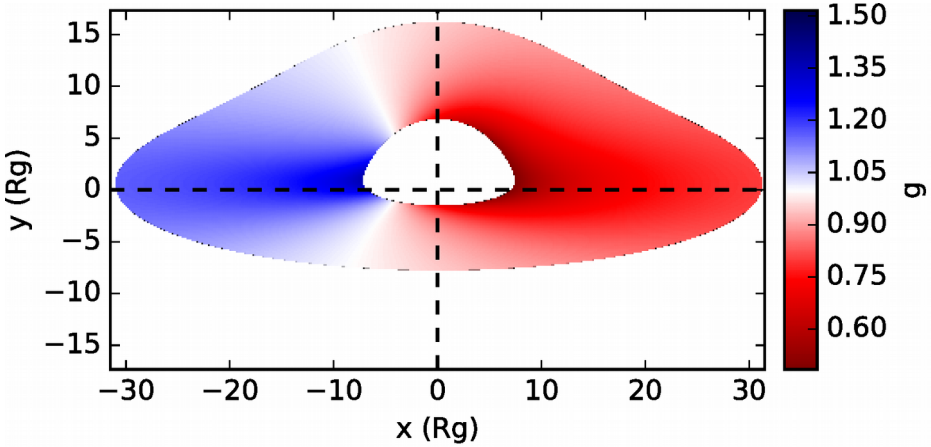
y (Rg)
x (Rg)
g
1.50
1.35
1.20
1.05
0.90
0.75
0.60

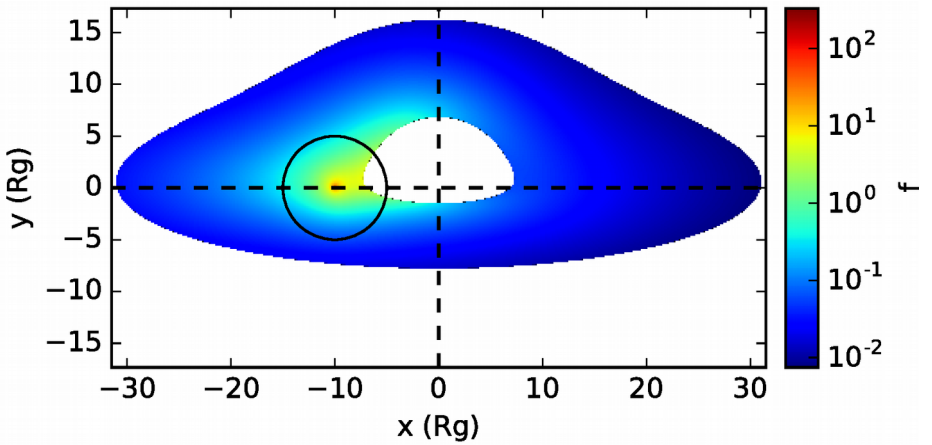
y (Rg)
x (Rg)
f

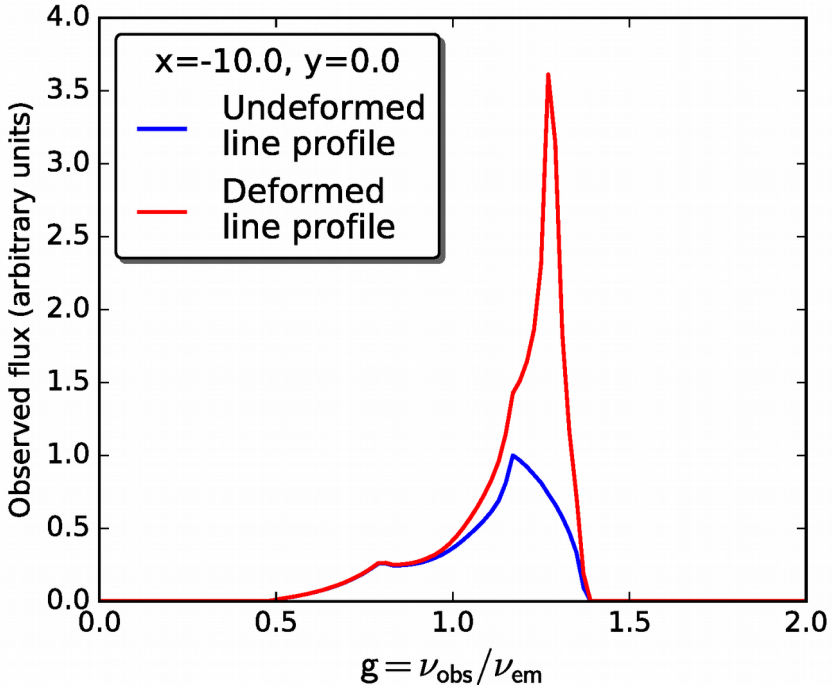
x=-10.0, y=0.0
Undeformed line profile
Deformed line profile
Observed flux (arbitrary units)
g = ν_obs / ν_em

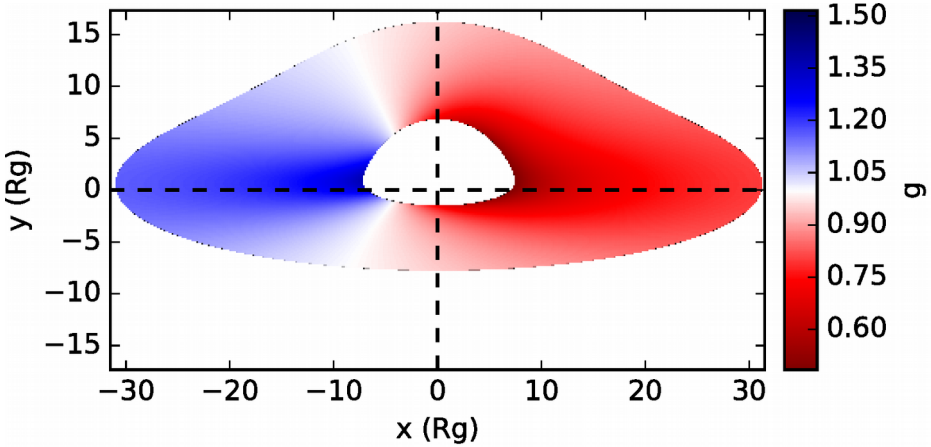
y (Rg)
x (Rg)
g
1.50
1.35
1.20
1.05
0.90
0.75
0.60

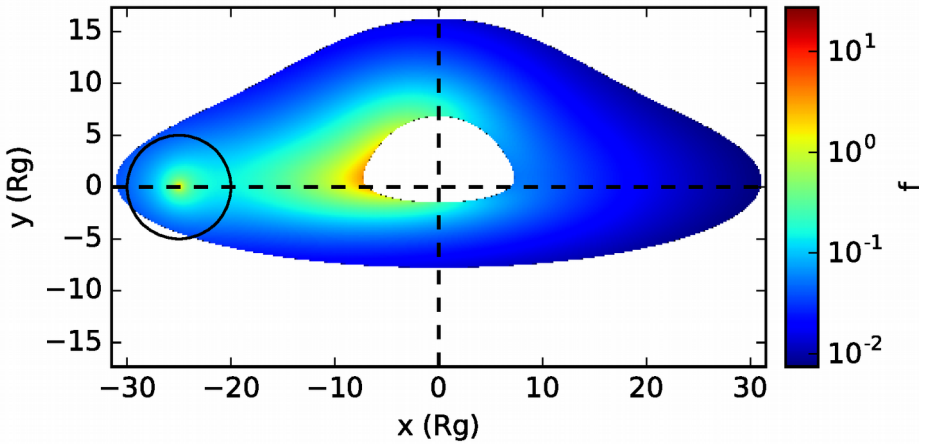
y (Rg)
x (Rg)
f

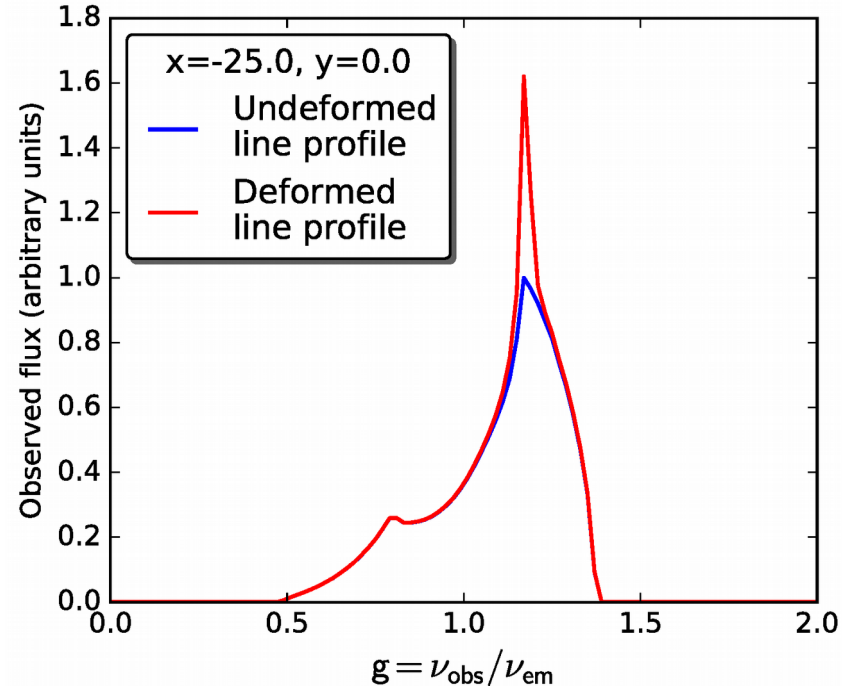
x=-25.0, y=0.0
Undeformed line profile
Deformed line profile
Observed flux (arbitrary units)
g = ν_obs / ν_em

Solution 2

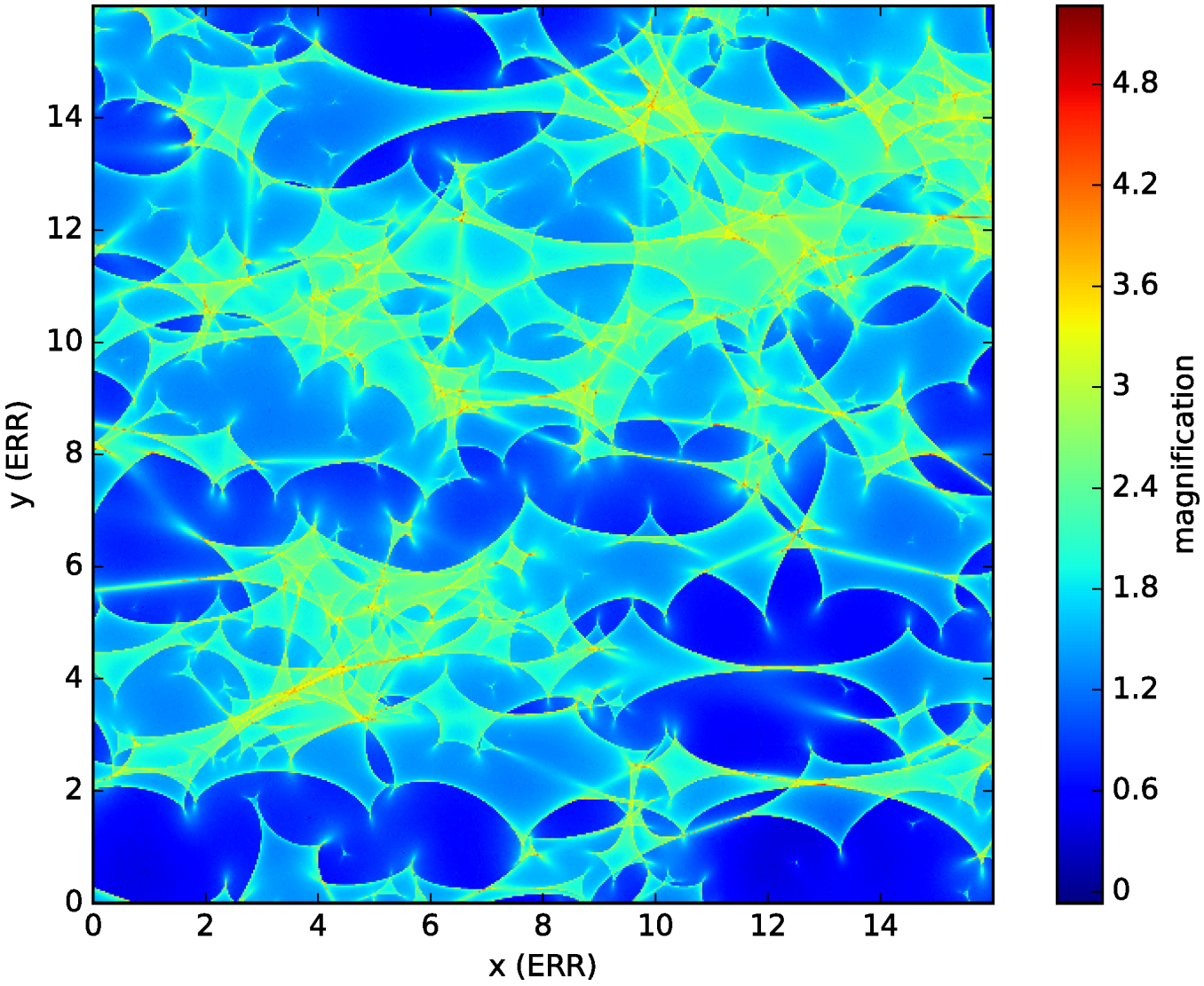

Input microlensing magnification map for a point-like source (solution is obtained by Python script "fits_view.py")

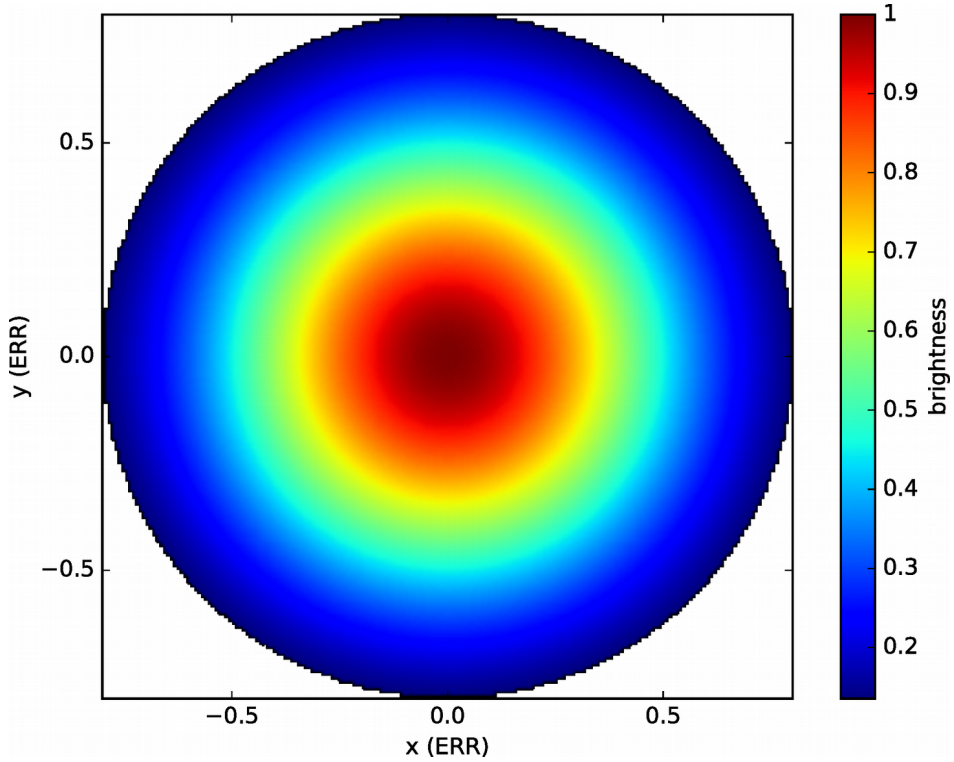

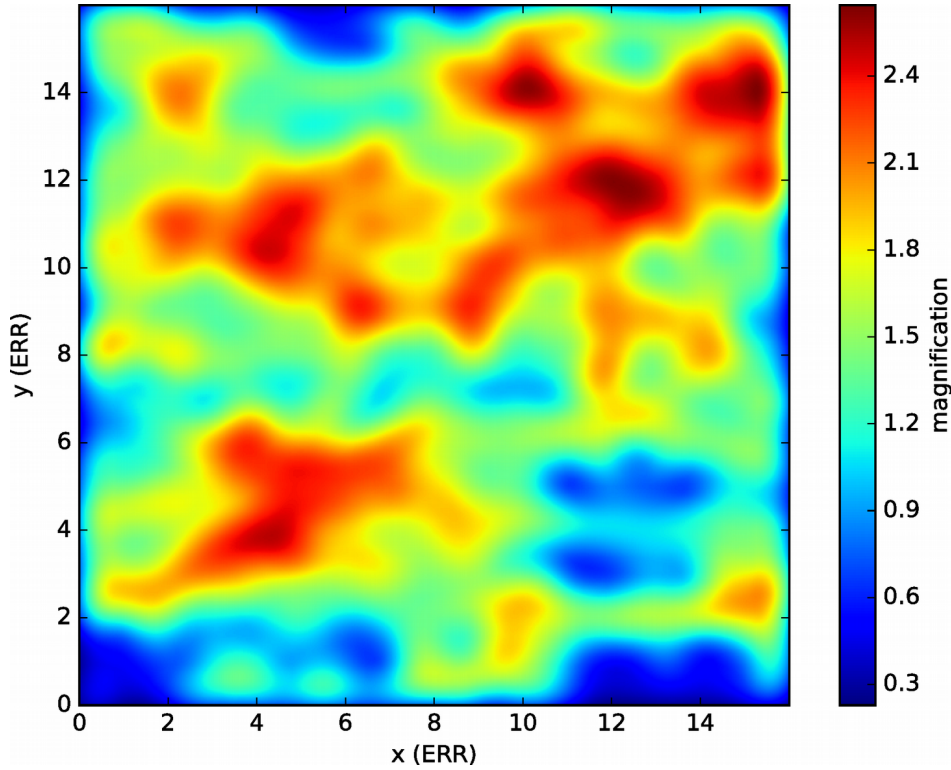

Extended circular source with Gaussian distribution of brightness for $\sigma = 0.4\ R_E$ (FITS file "source1.fits.gz")

The output magnification map (FITS file "mlmap_source1.fits.gz") after the convolution with the source in the left panel

Solution is obtained by Python script "circular_source.py"

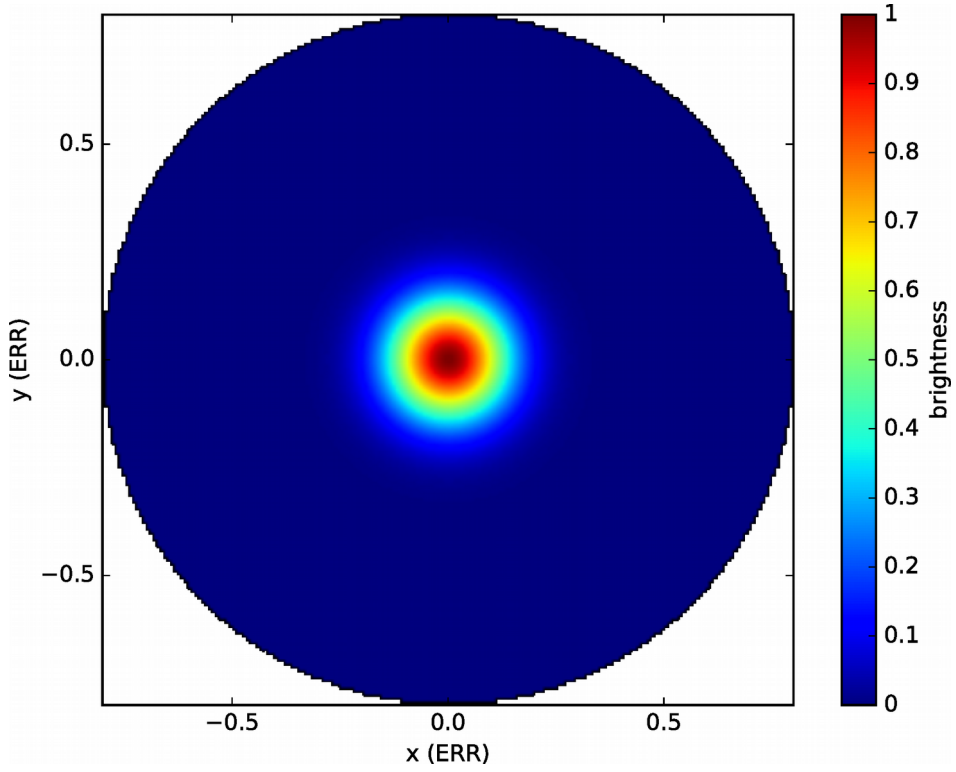

Extended circular source with Gaussian distribution of brightness for $\sigma = 0.1\ R_E$ (FITS file "source2.fits.gz")

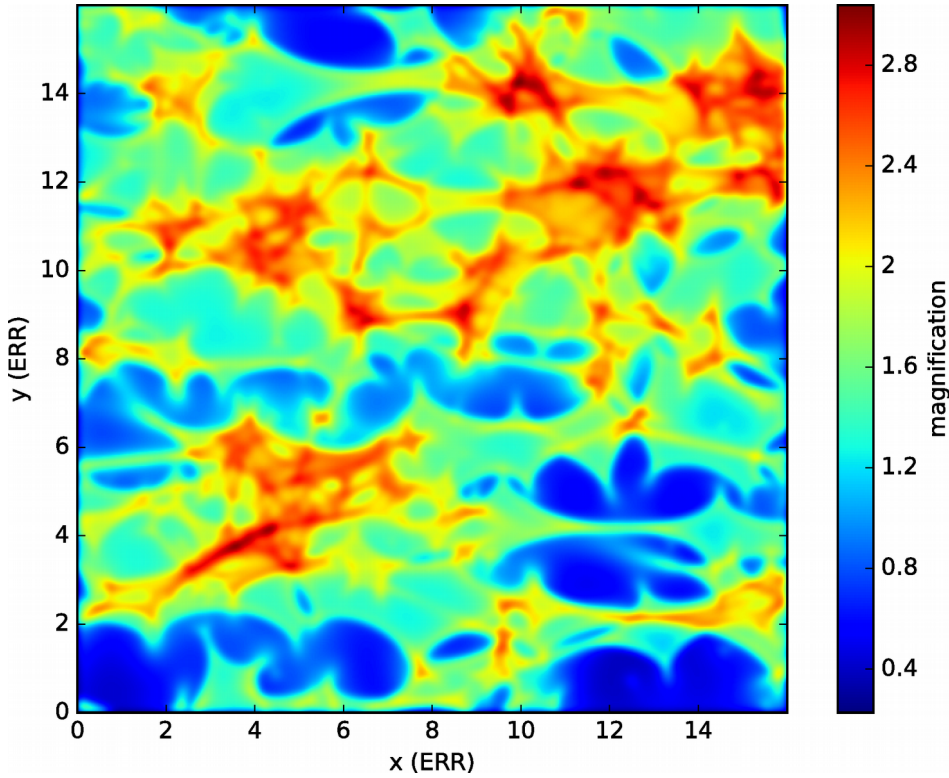

The output magnification map (FITS file "mlmap_source2.fits.gz") after the convolution with the source in the left panel

Solution is obtained by Python script "circular_source.py"

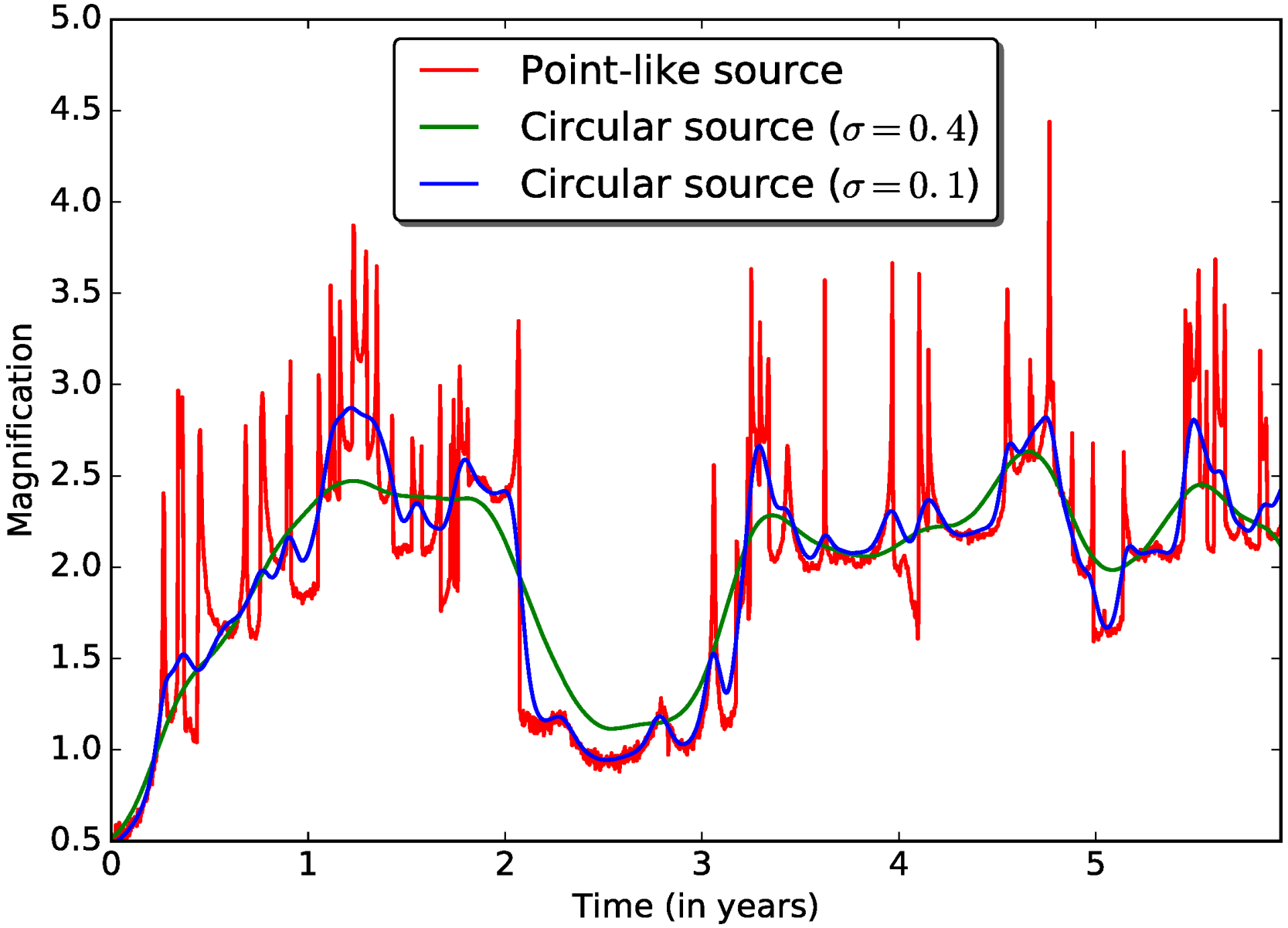

Simulated microlensing light curves (solution is obtained by Python script "light_curves.py")

Solution 3

Output of Python script "t_cross.py"

1. for a "typical" lens:

```
Enter the lens redshift: 0.5
Enter the source redshift: 2.0
Enter the source radius (in km): 1.5e+10
Enter the effective source velocity (in km/s): 600.0
Enter the Hubble constant (in km/s/Mpc): 75.0
Enter the Omega_matter: 0.3

Angular diameter distance of the lens: 1175.1 Mpc
Angular diameter distance of the source: 1611.5 Mpc
Microlensing crossing time 316.5 days
```

2. for Einstein Cross:

```
Enter the lens redshift: 0.04
Enter the source redshift: 1.695
Enter the source radius (in km): 1.5e+10
Enter the effective source velocity (in km/s): 600.0
Enter the Hubble constant (in km/s/Mpc): 75.0
Enter the Omega_matter: 0.3

Angular diameter distance of the lens: 152.3 Mpc
Angular diameter distance of the source: 1629.9 Mpc
Microlensing crossing time 28.1 days
```

Solution 4

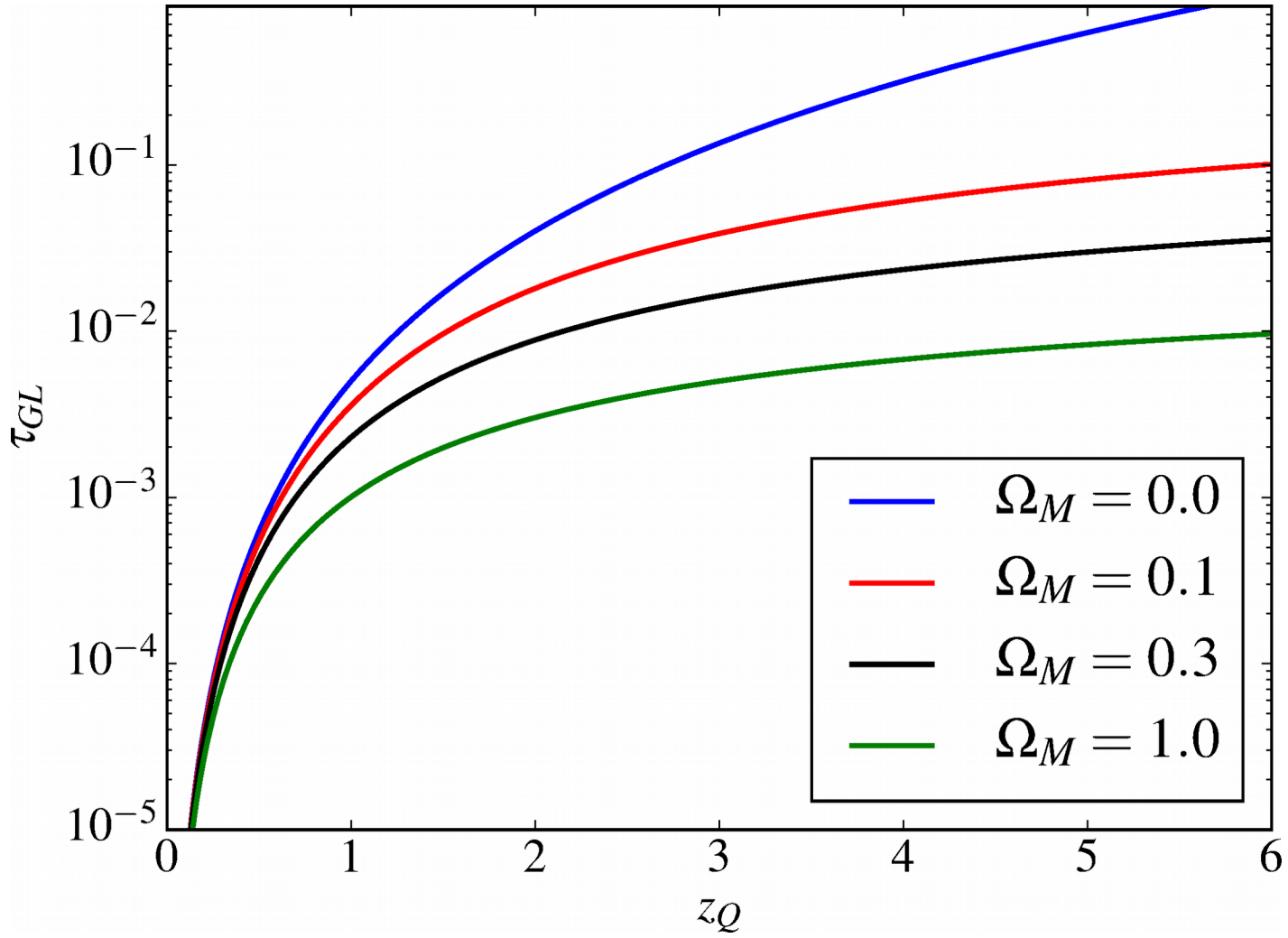

- $\tau_{\mathrm{GL}} \approx 0.01$ for a quasar at redshift $z_Q = 2$ in the case of $\Omega_M = 0.3$
- Solution is obtained by Python script "taugl.py"